

Electronic Thesis and Dissertation Repository

3-22-2018 8:30 AM

A Genetic Screen to Identify Fission Yeast Genes with Roles in Protecting Against Perturbation of the Actin Cytoskeleton

Dorota Michalski, *The University of Western Ontario*

Supervisor: Karagiannis, Jim, *The University of Western Ontario*

A thesis submitted in partial fulfillment of the requirements for the Master of Science degree in Biology

© Dorota Michalski 2018

Follow this and additional works at: <https://ir.lib.uwo.ca/etd>



Part of the [Genetics Commons](#), [Genomics Commons](#), and the [Molecular Genetics Commons](#)

Recommended Citation

Michalski, Dorota, "A Genetic Screen to Identify Fission Yeast Genes with Roles in Protecting Against Perturbation of the Actin Cytoskeleton" (2018). *Electronic Thesis and Dissertation Repository*. 5334. <https://ir.lib.uwo.ca/etd/5334>

This Dissertation/Thesis is brought to you for free and open access by Scholarship@Western. It has been accepted for inclusion in Electronic Thesis and Dissertation Repository by an authorized administrator of Scholarship@Western. For more information, please contact wlsadmin@uwo.ca.

Abstract

In the fission yeast, *Schizosaccharomyces pombe*, stress upon the cell division machinery leads to the activation of a cytokinesis checkpoint. This checkpoint results in a delay in cell cycle progression and the prolonged maintenance of a cytokinesis competent cellular state. In this state the cell is able to continuously reform/repair the actomyosin ring until cell division is achieved. To uncover genes that play a role in enforcing this checkpoint, the actin depolymerizing drug Latrunculin A (LatA) was used to perturb the cytokinetic machinery in a set of 3400 viable haploid *S. pombe* gene deletion mutants. Thirty-eight gene deletion mutants hypersensitive to LatA were identified in this screen. Among this set of genes, the transcription factor adhesion defective protein 2 (*adn2*) showed one of the strongest phenotypes in response to LatA and was thus characterized further. Interestingly, live-cell imaging experiments showed that *adn2* gene deletion mutants, while initially able to assemble the actomyosin ring, were unable to properly constrict the ring in the presence of LatA leading to cell division failure. Furthermore, over-expression experiments demonstrated that abnormally high levels of Adn2p result in morphological/cytokinetic phenotypes suggesting a possible dominant-negative effect.

Keywords: Fission yeast, Cell division, Cytokinesis, Cell cycle checkpoint, Latrunculin A, Actin, Actomyosin ring

Co-Authorship Statement

This thesis incorporates material that is the result of joint research between Dorothy Michalski and Farzad Asadi (under the supervision of Jim Karagiannis). F. Asadi and D. Michalski conducted the original LatA sensitivity screen in collaboration; with F. Asadi being primarily responsible for two of the three individual trials performed and D. Michalski being primarily responsible for a third individual trial. The subset of Latrunculin A mutants identified in the screen were further analyzed by spot assays, disk diffusion assays, minimum inhibitory concentration assays, and fluorescence microscopy. F. Asadi and D. Michalski divided this work with each being responsible for analyzing a subset of the gene deletion mutants. The data from all three trials was collated and published in the journal “G3: Genes, Genomes, Genetics” under the Creative Commons Attribution License (<https://creativecommons.org/licenses/by/4.0/>), which permits unrestricted use, distribution, and reproduction in any medium, provided the original work is properly cited, and whereby the authors (F. Asadi, D. Michalski, and J. Karagiannis) retain the copyright. Some passages have thereby been quoted verbatim from “A Genetic Screen for Fission Yeast Gene Deletion Mutants Exhibiting Hypersensitivity to Latrunculin A. Farzad Asadi, Dorothy Michalski and Jim Karagiannis. G3: GENES, GENOMES, GENETICS October 1, 2016 vol. 6 no. 10 3399-3408; <https://doi.org/10.1534/g3.116.032664>.” Figures 3-1 to 3-5 and Tables 3-1 to 3-3 of this thesis have also thereby been reproduced from the aforementioned work under the terms of the license. With respect to work involving the detailed characterization of the *adn2* gene deletion mutant, all experimental work, data analysis, interpretation, and writing was performed by Dorothy Michalski (under the supervision of J. Karagiannis).

Acknowledgments

I first acknowledge and thank my supervisor Dr. Jim Karagiannis for giving me the opportunity to complete my Master's degree in his lab. The continuous support and contribution he has made to my project has been invaluable.

I also acknowledge Farzad Asadi, without whom this project would not have not been possible. He provided a wealth of knowledge, support and understanding. His dedication to the project and his constant encouragement and suggestions were always welcome.

I thank my Advisory Committee, Dr. Kathleen Hill and Dr. Sashko Damjanovski, whose perspectives improved the caliber of my project.

I acknowledge my lab mate Ash Rayhan, for always having a listening ear, on topics of school and life, and for making the time spent waiting on experiments enjoyable.

Finally, I thank my friends and parents for their continuous support. To my parents, who have continuously supported my educational pursuits and for providing sound advice. And finally, to my friends for understanding when I would have to cancel plans and for helping me during stressful times.

Table of Contents

Abstract	i
Co-Authorship Statement.....	ii
Acknowledgments.....	iii
Table of Contents	iv
List of Tables	vii
List of Figures	viii
List of Appendices	ix
List of Abbreviations	x
Chapter 1	1
1 Introduction	1
1.1 A checkpoint system is required for the faithful execution of cytokinesis in <i>Schizosaccharomyces pombe</i>	1
1.2 Cytokinesis in eukaryotes	3
1.3 <i>Schizosaccharomyces pombe</i> as a model organism for studying cytokinesis.....	6
1.4 Cytokinetic mechanisms in <i>S. pombe</i>	7
1.5 Comparison of cytokinesis in <i>Schizosaccharomyces pombe</i> and animal cells	11
1.6 The cytokinesis checkpoint system.....	12
1.7 Using latrunculin A to screen for genes involved in the cytokinesis checkpoint .	13
1.8 Rationale	16
Chapter 2.....	17
2 Materials and Methods.....	17
2.1 Strains, media, and growth conditions	17
2.2 Primary screen	17
2.3 Spot assays	18

2.4	Disk diffusion assays	18
2.5	Minimum inhibitory concentration assays.....	19
2.6	Fluorescence microscopy.....	19
2.7	Molecular cloning.....	20
2.7.1	Creation of the pJK210- <i>adn2</i> -GFP construct.....	20
2.7.2	Creation of the pREP1- <i>adn2</i> , pREP41- <i>adn2</i> and pREP81- <i>adn2</i> over-expression constructs	21
2.8	Live cell imaging	21
2.9	<i>adn2</i> over-expression analysis	22
Chapter 3.....		23
3	Results	23
3.1	Primary screen	23
3.2	Secondary screening	27
3.3	Screening for cytokinesis mutants	33
3.4	Bioinformatical analysis of the <i>adn2</i> gene.....	36
3.4.1	Domain structure.....	36
3.4.2	Phylogenetic analysis.....	37
3.4.3	Protein interaction network.....	40
3.5	Live-cell imaging of cytokinesis in <i>adn2Δ</i> mutants.....	42
3.6	Over-expression analysis of the <i>adn2</i> gene	44
3.7	Intracellular localization of Adn2-GFP.....	46
Chapter 4.....		48
4	Discussion.....	48
4.1	Identifying cytokinesis checkpoint genes	48
4.2	Hypersensitive mutants show varying degrees of sensitivity to LatA	49
4.3	Adn2p is required for ring constriction upon LatA treatment	51

4.4 The Adn2p transcription factor localizes to the nucleus.....	52
4.5 Overexpression of And2p results in cytokinetic abnormalities	53
4.6 Adn2p might be part of a multi-protein complex with roles in defending against cytoskeletal perturbations	53
4.7 Adn2p target genes include cell wall remodeling enzymes.....	56
4.8 Future work concerning the role of Adn2p in defending against cytoskeletal perturbations	58
Literature Cited	60
Appendices.....	67
Curriculum Vitae	79

List of Tables

Table 3-1 Ranking of the LatA sensitivity of each gene deletion mutant based on linear regression analysis of data plotting the area of the zone of inhibition (pixels) vs. LatA concentration (μM)	31
Table 3-2 Minimum inhibitory concentration of latrunculin A for the indicated gene deletion mutants	32
Table 3-3 Mean percentage of cells (+/- SD) displaying the indicated phenotype after 5 hours treatment with 0.3 μM Latrunculin A (n=3)	35

List of Figures

Figure 1-1 Cytokinesis in the fission yeast, <i>S. pombe</i> , and in animal cells.	4
Figure 1-2 Cytokinesis in <i>S. pombe</i>	9
Figure 1-3 Cellular phenotypes upon LatA treatment	15
Figure 3-1 Overview of the genetic screen described in this thesis	24
Figure 3-2 Primary screen.....	26
Figure 3-3 Spot assays	28
Figure 3-4 Disk diffusion assays.....	30
Figure 3-5 The gene deletion mutants of the high-confidence list are prone to cytokinesis failure in the presence of Latrunculin A	34
Figure 3-6 Domain Structure of Adn2p	38
Figure 3-7 Phylogenetic analysis of Adn2p and its related proteins.....	39
Figure 3-8 Protein interaction network of the Adn2p protein.....	41
Figure 3-9 Actomyosin ring integrity in <i>adn2Δ</i> mutants	43
Figure 3-10 Overexpression analysis of Adn2p.....	45
Figure 3-11 Intracellular localization of Adn2p	41

List of Appendices

Appendix A: Complete list of LatA sensitive gene deletion mutants identified via genome-wide screening.	67
Appendix B: CLUSTAL O (1.2.4) multiple sequence alignment.....	74

List of Abbreviations

Adn: Adhesion defective

Atg: Autophagy

Byr: Bypass of yeast Ras

Cdc: Cyclin-dependent protein kinase

Cdr: Changed division response

Cvt: Cytoplasm to vacuole targeting

DAPI: 4',6-diamidino-2-phenylindole

DMSO: Dimethyl sulfoxide

EMM: Edinburgh minimal medium

FLO: Flocculation

GFP: Green fluorescent protein

LatA: Latrunculin A

LB: Lysogeny broth

LisH: LIS1 homology

MIC: Minimum inhibitory concentration

Mid: Medial ring

Pap1: Pombe AP-1

PAS: Phagophore assembly site

PBS: Phosphate buffered saline

PCR: Polymerase chain reaction

Plo: Polo kinase

Rlc: Regulatory light chain

Sid: Septation initiation-deficient

SIN: Septation initiation network

SPAS: Sporulation agar

ssDP: single-stranded DNA binding protein

Spg: Septum-promoting GTPase

Thia: Thiamine

YES: Yeast extract with supplements

Chapter 1

1 Introduction

1.1 A checkpoint system is required for the faithful execution of cytokinesis in *Schizosacharomyces pombe*

Cytokinesis is the final step of the cell cycle in which a cell divides to give rise to two daughter cells, each containing a full genomic complement and an equal distribution of organelles (Fededa & Gerlich, 2012). The faithful and reliable execution of cytokinesis is carefully monitored and depends on the coordination of numerous spatial and temporal events (Balasubramanian et al., 2004). For example, cytokinesis must be spatially regulated to occur only between segregated chromosomes. It must also be temporally regulated to occur after mitosis to ensure a full DNA complement is segregated to each daughter cell. Failure of proper spatial and temporal regulation of cytokinesis can compromise genomic integrity and negatively impact cell viability (Prekirs & Gould, 2008).

The association between cytokinesis failure and cell viability was first described in Theodore Boveri's 1914 work 'Concerning the Origin of Malignant Tumours'. In his work, Boveri links cytokinesis failure and the resulting genomic instability with tumour development. Boveri hypothesized that a consequence of cytokinesis failure was the formation of tetraploid cells, which in addition to containing extra chromosomes, also contain extra centrosomes. The presence of multiple centrosomes renders the transient tetraploid cells susceptible to undergoing a chaotic multipolar mitosis (as opposed to a bipolar mitosis) in which chromosomes are mis-segregated as a result of being pulled to

multiple poles. The cells resulting from this chaotic multipolar mitosis are genetically unstable aneuploids. Due to additional or missing chromosomes these cells are more likely to become malignant (Harris et al., 2008). The direct link between cytokinesis failure and genomic integrity emphasizes the importance of understanding the mechanisms that ensure the faithful and reliable execution of cytokinesis.

Today it is clear that aneuploidy is a common feature of human cancers. Furthermore, numerous experiments support Boveri's hypothesis that cytokinetic failure leads to tumour formation (Olaharski et al., 2006; Ganem et al., 2007; Holland & Cleveland, 2009). In one experiment, diploid mouse ovarian surface epithelial cells that had failed in cytokinesis were observed to experience an intermediate tetraploid stage before evolving to aneuploidy. Injection of the aneuploid cells into mice resulted in tumour formation at the site of injection (Lv et al., 2012).

Additional experiments have identified tumour suppressor proteins such as BRCA2 and p53 that are required for the faithful completion of cytokinesis (Daniels et al., 2004; Fujiwara et al., 2005). While research has established a direct relationship between cytokinesis failure and tumour formation, our understanding of the mechanisms in place for the faithful and reliable execution of cytokinesis is lacking (Karagiannis, 2012). An understanding of the mechanisms required for the successful completion of cytokinesis is important as it can deepen our understanding of basic eukaryotic cell biology and provide insight into mammalian tumour development.

1.2 Cytokinesis in eukaryotes

Much of our understanding of cytokinesis comes from experiments using model organisms. Organisms amenable to genetic manipulation such as *Saccharomyces cerevisiae*, *Drosophila melanogaster*, and *Schizosaccharomyces pombe* have served as powerful tools in elucidating the components of cytokinesis. In animal cells, cytokinesis normally proceeds through a series of tightly coordinated and regulated steps beginning with specification of the cleavage plane, formation and constriction of the actomyosin ring, and finishing with the physical separation of the two cells (Fededa & Gerlich, 2012). The major events of cytokinesis are conserved among organisms, and this is particularly evident when comparing animal cell and fission yeast cytokinesis (Pollard & Wu, 2010) (**Figure 1-1**).

In animal cells the site of cell division and future contractile ring assembly is determined during anaphase by the mitotic spindle after sister chromatid separation (Eggert et al., 2006; Barr & Grueneberg, 2007). During early anaphase, kinetochore microtubules attach to the kinetochore of a chromosome, driving the segregation of sister chromatids to opposite spindle poles. Once chromosomes have been separated to opposite halves of the cell, polar microtubules emanating from opposite spindle poles compact into overlapping, antiparallel bundles to form the central spindle. The central spindle serves as a regulating center for cytokinesis by recruiting proteins necessary for cleavage furrow positioning and future abscission (Glotzer, 2001; Guertin et al., 2002).

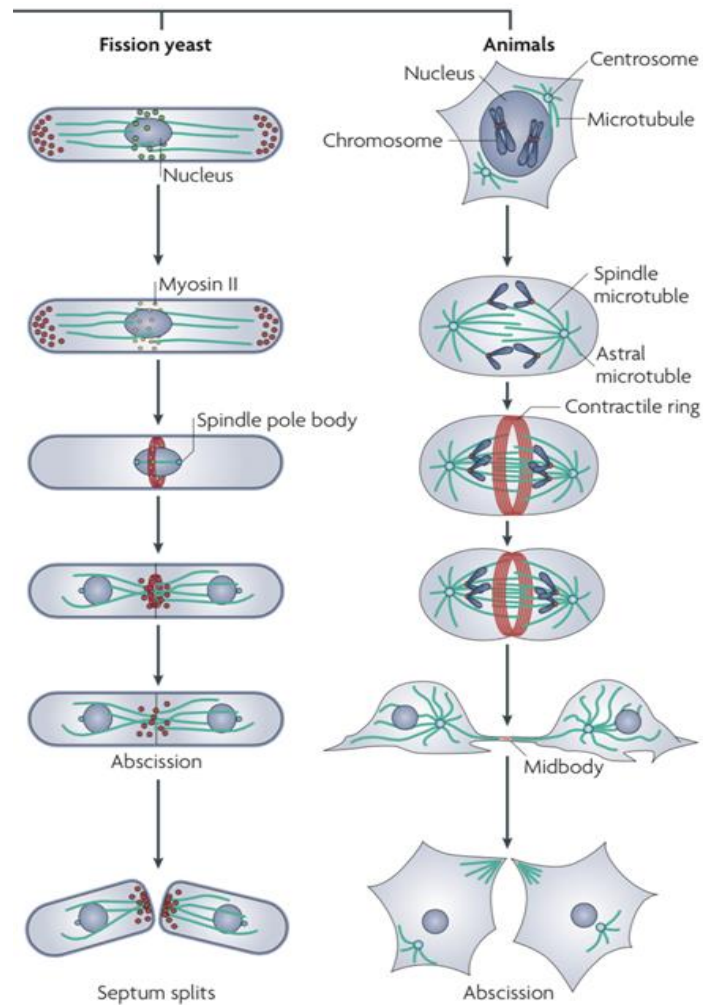


Figure 1-1. Cytokinesis in the fission yeast, *S. pombe*, and in animal cells. Both animal cells and *S. pombe* divide via medial fission using an actin and myosin based contractile ring. Specification of the division plane occurs during G2 in *S. pombe* and during anaphase in animal cells. Reproduced from Pollard & Wu (2010) under the fair use provision of the Canadian Copyright Modernization Act (2012).

The actomyosin ring is positioned in the medial region of the cell and constricts to create an indentation on the cell surface known as the cleavage furrow. As the actomyosin ring constricts the furrow ingresses and drags the plasma membrane inward, partitioning one cell into two daughter cells. Ring constriction also compresses the microtubules of the spindle midzone into a transient, narrow intracellular bridge known as the spindle midbody that connects the two cells for a short period. In the final step of cytokinesis, the midbody recruits proteins required for abscission and vesicles deliver newly synthesized membrane material to the midbody (Guertin et al., 2002; Glotzer, 2005).

Like animal cells, cytokinesis in *S. pombe* relies on the formation and constriction of an actomyosin ring in the medial region of the cell to complete cytokinesis (Simanis, 1995). Unlike animal cells, *S. pombe* is surrounded by a cell wall, which requires the deposition of a polysaccharide septum concomitant with ring constriction. The eventual degradation of the septum causes cell scission (Balasubramanian et al., 2004). Both animal cells and *S. pombe* have mechanisms in place to ensure that ring constriction does not occur prior to chromosome segregation, as mis-segregation of chromosomes can disrupt genomic integrity (Glotzer & Simanis, 1997; Glotzer 2001; Guertin et al., 2002). Currently, we do not have a thorough understanding of the mechanisms that ensure the faithful and reliable execution of cytokinesis and therefore require further research to deepen our understanding (Karagiannis, 2012).

1.3 *Schizosaccharomyces pombe* as a model organism for studying cytokinesis

The elucidation of cell cycle control mechanisms in fission yeast by Nobel laureate Paul Nurse made *S. pombe* a commonly used model organism for the study of diverse biological processes, most notably the cell cycle (Nurse et al., 1976, Nurse & Thuriaux., 1980, Lee & Nurse, 1987). In particular *S. pombe* has been used to research eukaryotic cytokinesis since the basic mechanisms of cytokinesis and general order of events are shared between *S. pombe* and animal cells (Wolfe & Gould, 2005). Both use a contractile actomyosin ring to divide, share most genes used in cytokinesis and both have regulatory mechanisms in place to ensure cytokinesis occurs after mitosis (Balasubramanian et al., 2004). The conservation of these basic mechanisms in cytokinesis should provide insights into cytokinesis in other organisms (Pollard & Wu, 2010).

In addition to the shared similarities with human cells, *S. pombe* is also genetically tractable (Balasubramanian et al., 2004). *S. pombe* has a simple haploid genome on three chromosomes that have been fully sequenced and annotated (Wood et al., 2002). Due to the relatively simple genome, deletion strains are available for 98% of the ~4900 total genes in *S. pombe*. Furthermore, many cytokinesis proteins have been tagged with fluorescent markers. Finally, a large number of cytokinesis defective mutants have been identified in *S. pombe* (Karagiannis, 2012).

1.4 Cytokinetic mechanisms in *S. pombe*

The execution of cytokinesis in *S. pombe*, just as in more complex eukaryotes, relies on the formation and constriction of an actomyosin ring in the medial region of the cell. In *S. pombe* the position of the interphase nucleus determines the location of the future division site (Guertin et al., 2002). The position of the actomyosin ring is coupled to nuclear position via the nuclear export of anillin-like nuclear protein, Mid1p, in a Plo1p-dependent manner (Bahler & Pringle, 1998; Daga & Chang, 2005). Mid1p localizes to the cortex overlying the nucleus, marking the future division site (**Figure 1-2**). Mid1p also serves as a spatial cue for the recruitment of ring components to the medial region during interphase (Bahler & Pringle, 1998; Daga & Chang, 2005; Huang et al., 2007). These protein clusters in the medial region of the cell are known as interphase nodes and represent the first step in actomyosin ring assembly (Guertin et al., 2002). Additional proteins including Wee1p, Cdr1p and Cdr2p also localize to interphase nodes at the onset of mitosis (Wu & Pollard, 2005; Bathe & Chang, 2010; Almonacid & Paoletti, 2010).

Interphase nodes are restricted to the middle of the cell by the kinase Pom1p, which forms a polar gradient at both ends of the cell (Celton-Morizur et al., 2006; Moseley et al., 2009). As the cell grows lengthwise during G2, the levels of Pom1p in the middle of the cell decrease, triggering mitosis by releasing inhibition of Cdr1p and Cdr2p kinases. Cdr1p and Cdr2p negatively regulate the kinase Wee1p through phosphorylation. When phosphorylated, Wee1p is no longer able to inhibit the cyclin dependent kinase, Cdc2p, which controls cell cycle progression. Release of Cdc2p inhibition by Wee1p triggers the transition from G2 into mitosis and occurs

coincidentally with chromosome segregation (Morgan, 1997). This system ensures that ring assembly is tightly coordinated with mitotic entry and does not initiate before chromosomes have been segregated (Guertin et al., 2002).

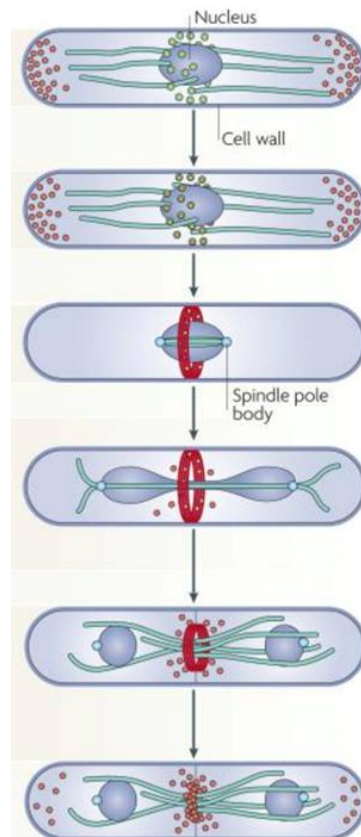


Figure 1-2. Cytokinesis in *Schizosaccharomyces pombe*. Mid1p localizes to the cell cortex overlying the nucleus where it recruits ring components to the median in clusters known as interphase nodes (green circles). The interphase nodes mark the site for future actomyosin ring assembly. The polymerization of actin filaments by Cdc12p and maturation of interphase nodes into cytokinesis nodes is followed by node compaction into a tightly bundled ring (shown in red). SIN signaling initiates ring constriction and septum assembly. Actin patches are shown as pink circles. Microtubules are shown as green filaments. Reproduced from Pollard and Wu (2010) under the fair use provision of the Canadian Copyright Modernization Act (2012).

Once the cell has entered mitosis, interphase nodes mature into cytokinesis nodes through the addition of myosin II and the ring proteins, Rng2p (ring assembly protein), Cdc15p, and Cdc12p (Moseley et al., 2009). Actin is assembled into the ring by the formin Cdc12p, which interacts with actin monomers, aiding their polymerization into filaments. Tropomyosin and fimbrin then condense the actin into a compact ring (Kovar et al., 2003; Wu & Pollard, 2005; Wu et al., 2006).

Once the ring is formed, the timing of its constriction and the initiation of cytokinesis are coordinated to occur with the completion of the preceding mitosis (Wolfe & Gould, 2005). In *S. pombe*, ring constriction and septum formation is controlled by a kinase signaling cascade known as the Septation Initiation Network (SIN) (Simanis, 1995; Krapp & Simanis, 2008). Components of the SIN assemble at the spindle pole body, the *S. pombe* counterpart of the mammalian centrosome (Hou et al., 2000). The SIN signaling cascade consists of three kinases, Cdc7p, Sid1p, and Sid2p, along with the small GTPase, Spg1p. Sid4p and Cdc11p are scaffold proteins that remain at the SPB during all cell cycle stages and anchor the SIN kinases to the SPB during mitosis (Krapp & Simanis, 2008). The small GTPase Spg1p controls SIN signal transduction. During interphase Spg1p remains at the SPB, bound to Byr4p-Cdc16p in its inactive GDP bound form, inhibiting SIN signaling and thereby preventing septation from occurring during interphase. During metaphase, decreasing levels of Cdc16p allow Spg1p to dissociate from the Byr4p-Cdc16p complex. In its now active GTP-bound form, Spg1p recruits Cdc7p to the SPB. This leads to the recruitment of Sid4p-Cdc11p to the SPB. The recruitment of Sid4p-Cdc11p to the SPB causes Sid2p-Mob1p to re-localize from the SPB to the site of cell division to initiate

ring constriction and division septum formation. Degradation of the septum and release of the two daughter cells completes cytokinesis (Schmidt et al., 1997; Tomlin et al., 2002; Mishra et al., 2005).

1.5 Comparison of cytokinesis in *Schizosaccharomyces pombe* and animal cells

The major events of cytokinesis include cleavage plane specification, rearrangement of the cytoskeleton/microtubules, contractile ring assembly, constriction, and abscission. In general, the major events of cytokinesis are conserved in *S. pombe* and animal cells, although structural and regulatory differences between the two require the utilization of different strategies to complete cytokinesis (Balasubramanian et al., 2004).

One of the earliest steps in cytokinesis is specification of the division plane – the site of future actomyosin ring formation and cell division (Almonacid & Paoletti, 2010). To ensure equal partitioning of genomic and cytoplasmic content, most eukaryotes position the division plane perpendicular to the axis of chromosome segregation in the medial region of the cell (Eggert et al., 2006). However, the mechanism and timing of division plane specification varies between fission yeast and animal cells. In animal cells the cleavage plane is determined during anaphase and reflects the position of the mitotic spindle. In fission yeast the future site of cell division is determined in G2 by the position of the interphase nucleus (Balasubramanian et al., 2004; Gould, 2005).

Both mammalian and fission yeast divide by the formation and constriction of an actomyosin ring. In both organisms, actin and myosin are used to contract the ring

(May, 1997; Kitayama, 1997). The basic composition of the ring in animal and *S. pombe* cells is very similar, and many conserved families of proteins required for ring assembly are common to both organisms such as actin, myosin II, and formins (Bezanilla et al., 1997; Wu, 2002; Pollard & Wu, 2010). While many of the components that make up the actomyosin ring are conserved, the timing of ring assembly is different. In *S. pombe* components required for ring assembly localize to the medial region in G2, although ring assembly occurs once the cell enters mitosis (Balaubramanian et al., 2004). In animal cells actomyosin ring assembly occurs closer to the end of mitosis, during anaphase (Rappoport, 1996, Glotzer, 2001).

At the end of cytokinesis, the cell must ensure that daughter cells receive an equal amount of cytoplasmic material and proteins, which requires an increase in cell volume. In animal cells membrane material is added or redistributed during cytokinesis (Glotzer, 2005). In *S. pombe* the presence of a cell wall requires the deposition of a polysaccharide septum as the ring constricts (Wolfe & Gould, 2005). The majority of the surface area required for both daughter cells is generated during interphase when the cell is undergoing polarized growth. During cytokinesis only the relatively narrow membrane and cell wall material that divides the cell during abscission must be added (Balasubramanian et al., 2004).

1.6 The cytokinesis checkpoint system

Progression through the cell cycle in *S. pombe* is monitored by cell cycle checkpoints. As the cell progresses through the phases of the cell cycle, checkpoints ensure completion of one phase prior to the initiation of a subsequent phase (Hartwell & Weinert, 1998). Checkpoint failure results in abnormal progression through the cell

cycle and ultimately renders cells inviable. For example, the SIN ensures that cytokinesis begins only once the preceding mitosis is complete and chromosomes have been equally segregated. Recently there has been evidence of a cytokinesis monitoring checkpoint in *S. pombe* which ensures cytokinesis completion prior to the initiation of the subsequent mitosis (Krapp & Simanis, 2008; Karagiannis, 2012).

Evidence of a cytokinesis checkpoint can be observed when the cytokinetic machinery is mildly stressed. Under these conditions cells are held in a prolonged cytokinesis competent state during interphase and will delay entry into the next round of mitosis to give the cell time to stabilize/re-establish the actomyosin ring (Liu et al., 2000; Le Goff et al., 1999; Trautmann et al., 2001; Mishra et al., 2004; 2005). Evidence of a cytokinesis checkpoint comes from the characterization of cytokinesis mutants – that when exposed to mild perturbation to their cytokinetic machinery – are incapable of arresting the cell cycle or maintaining a prolonged cytokinesis competent state. As a result, these cells do not complete cytokinesis (Le Goff et al., 1999; Liu et al., 2000; Trautmann et al., 2001). The cytokinesis checkpoint involves the SIN, the Clp1p phosphatase, and the 14-3-3 protein Rad24p (Liu et al., 2000; Karagiannis et al., 2005; Mishra et al., 2005; Karagiannis, 2012).

1.7 Using latrunculin A to screen for genes involved in the cytokinesis checkpoint

Genes with a role in the cytokinesis checkpoint can be identified by screening gene deletion mutants with the actin depolymerizing drug Latrunculin A (LatA). LatA is a toxin produced by the Red Sea Sponge. It sequesters actin monomers, preventing their polymerization into a filamentous structure (Ayscough et al., 1997). In this way

LatA treatment inhibits assembly of the actomyosin ring. LatA has commonly been used in experiments at high concentrations (10-50 μM) to completely disrupt the actomyosin ring. However, LatA can also be used in low doses (0.2 – 0.5 μM) to mildly stress the cytokinetic machinery (Ayscough, 1997). This activates the cytokinesis checkpoint system to prolong cytokinesis as the cell attempts to reform/repair the actomyosin ring (Ayscough et al., 1997; Mishra et al., 2004; 2005).

Upon treatment with low dose LatA, mutants bearing deletions in genes critical to the cytokinesis checkpoint are unable to arrest the cell cycle or maintain a cytokinesis competent state in order for the cell to re-establish the actomyosin ring. The inability to delay entry into the next round of mitosis causes continuous rounds of nuclear division in the absence of cytoplasmic division and results in elongated, multinucleated cells with a fragmented septum (Wolfe & Gould, 2005) (**Figure 1-3**). Wild-type cells, however, are able to delay entry into the subsequent mitosis upon mild perturbation of the cytokinetic machinery. A functional cytokinesis checkpoint ensures that cytokinesis is complete prior to entry into the subsequent round of mitosis, resulting in successful cell division (Karagiannis et al., 2005; Mishra et al., 2005). Analysis of these mutants can therefore allow us to better understand the molecular mechanisms underlying the cytokinesis checkpoint.

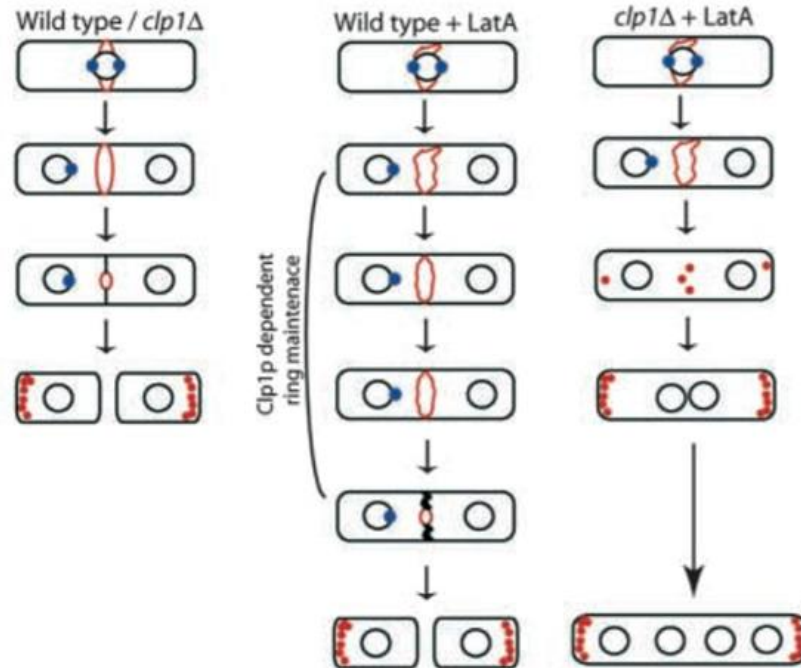


Figure 1-3 Cellular phenotypes upon LatA treatment. Both wild-type cells and cytokinesis checkpoint mutants (e.g. *clp1Δ*) are able to complete cytokinesis under normal growth conditions (left panel). Upon treatment with low doses of LatA, wild-type cells can delay entry into mitosis through activation of the cytokinesis checkpoint, which maintains a cytokinesis competent state (middle panel). Cytokinesis checkpoint mutants are unable to activate this checkpoint upon mild perturbation of the actomyosin ring and cannot delay mitosis until cytokinesis is completed. As a result, cells are elongated and multinucleated (right panel). The actomyosin ring is shown as a red circle. Actin patches are shown as red dots. The nucleus is shown as a black circle. The spindle pole body (active) is shown as a blue dot. Reproduced from Karagiannis et al. (2004) under the fair use provision of the Canadian Copyright Modernization Act (2012).

1.8 Rationale

While a variety of mutants hypersensitive to LatA have been isolated and characterized (Karagiannis et al. 2005; Karagiannis and Balasubramanian, 2007; Saberianfar et al., 2011; Grewal et al., 2012; Rentas et al., 2012), a global assessment of the regulatory modules needed to respond to LatA-mediated perturbation is lacking. The Bioneer deletion mutant library (Kim et al., 2010) was thus used to identify genes that play a role in defending against LatA-induced stress on a genome-wide scale. To perform the genome-wide screen, strains were treated with 0.4 μM LatA, as this concentration is close to the dissociation constant for LatA, and only mildly disrupts the actin cytoskeleton. In this way the regulatory modules needed to mitigate the detrimental effects of abnormal cytoskeletal perturbations could be identified. In addition to the genome-wide screen, the detailed characterization of one of the identified genes, *adn2*, is presented as part of this thesis.

Chapter 2

2 Materials and Methods

2.1 Strains, media, and growth conditions

Schizosaccharomyces pombe strains used in this study were obtained from the commercial supplier (Bioneer Corporation) or from the Karagiannis laboratory collection. Unless stated otherwise, strains were cultured to mid-log phase (OD_{600} between 0.2-0.6) in yeast extract medium (YES) with supplements (adenine, histidine, leucine, and uracil) at 30°C with shaking at 150 rpm. Strains carrying auxotrophic markers were grown in Edinburgh minimal media (EMM) with supplements (uracil, adenine, histidine and/or leucine). To induce mating, strains were cultured in sporulation medium with supplements (SPAS) (Forsburg and Rhind, 2006). NEB 5-alpha competent *Escherichia coli* strains were used for molecular cloning experiments. Cells were made competent for transformation by placing them on ice for 30 minutes, followed by heat shock at 42°C for 30 seconds. After transformation, cells were grown on solid Lysogeny broth (LB) agar media with 100 µg/ml ampicillin, at 37°C.

2.2 Primary screen

An individual trial of the screen was performed using version 4 of the Bioneer genome-wide deletion mutant library. The library consists of 3400 haploid gene deletion mutants comprising ~ 95.3% of non-essential *S. pombe* genes. Each strain carries a defined gene deletion constructed with the *kanMX4* cassette (Kim et al. 2010). To assay LatA sensitivity, the gene deletion mutants were grown in 96-well microtiter plates in liquid YES medium (Forsburg and Rhind, 2006) at 30°C. Five microliter

aliquots were then spotted onto YES-agar medium containing 0.4 μM Latrunculin A (Focus Biomolecules) or YES-agar media containing an equivalent volume of DMSO (solvent control). The growth of the strains on LatA plates (relative to DMSO controls) was assayed visually after 3 days at 30°C. Results of the screen were collated with two other trials (performed by collaborator, F. Asadi). Hits were categorized into three groups: a “high-confidence” group consisting of gene deletion mutants that were scored as sensitive in each of the three trials, a “medium-confidence” group consisting of gene deletion mutants that were scored as sensitive in two of the three trials, and a “low-confidence” group consisting of gene deletion mutants that were scored as sensitive in only one of the three trials.

2.3 Spot assays

The respective gene deletion mutants of the high-confidence group were grown overnight at 30°C in liquid YES medium to an OD_{600} of 0.5. Five microliters of undiluted culture, as well as four ten-fold serial dilutions (made in liquid YES), were then spotted onto YES-agar plates containing DMSO (solvent control) or 0.1 μM , 0.2 μM , or 0.3 μM LatA. Growth was assayed visually after the plates had been incubated for four days at 30°C.

2.4 Disk diffusion assays

The respective gene deletion mutants of the high-confidence group were grown overnight at 30°C in liquid YES medium to an OD_{600} of 0.5. Cells at a concentration of 10^5 cells/mL were then mixed with molten YES-agar (~40°C) and poured into Petri dishes. Five microliters of DMSO (solvent control), or 2.2 μM , 4.4 μM , or 6.6 μM

LatA, were then spotted onto sterile filter paper disks (Whatmann No. 1) which were subsequently placed onto the surface of the respective YES-agar plates. Photographs were taken using a Fluor Chem SP imager after the plates had been incubated for four days at 30°C. The area of the zone of inhibition for each disk was measured using ImageJ software (<https://imagej.nih.gov/ij/>). The area of the zone of inhibition for each disk (measured in pixels) was then plotted against LatA concentration. The slope of the linear regression line was calculated using Microsoft Excel.

2.5 Minimum inhibitory concentration assays

The respective gene deletion mutants of the high-confidence group were grown overnight at 30°C in liquid YES media to an OD₆₀₀ of 0.5. Approximately 10⁵ cells of each mutant strain was then seeded into the wells of a 96-well microtiter plate containing 100 µL of YES medium with 0 µM, 0.025 µM, 0.05 µM, 0.075 µM, 0.1 µM or 0.2 µM LatA. The plates were incubated for 4 days at 30°C. The minimum inhibitory concentration was determined by visually inspecting the plates to ascertain the lowest concentration of LatA that prevented visible growth.

2.6 Fluorescence microscopy

The respective gene deletion mutants of the high-confidence group were grown overnight at 30°C in liquid YES medium to an OD₆₀₀ between 0.2 and 0.6. The cultures were then treated with DMSO or 0.3 µM LatA for five hours. Cells were fixed with two volumes of ice-cold ethanol and then spun at 5000 rpm for two minutes and re-suspended in 1 mL of PBS (pH 7.4) containing 1% Triton X-100. Cells were washed three times in PBS before being re-suspended in 100 µL of PBS containing 15%

glycerol. To observe nuclei and cell wall/septa material, cells were mixed with 0.02 mg/mL 4',6-diamidino-2-phenylindole (DAPI) and 1 mg/mL aniline blue. Fluorescence images (DAPI filter set) were obtained with a Zeiss Axioskop 2 microscope attached to a Scion CFW Monochrome CCD Firewire Camera (Scion Corporation, Frederick Maryland). The microscope system was driven by ImageJ 1.41 software (National Institutes of Health).

2.7 Molecular cloning

Molecular cloning was performed using New England Biolabs 5-alpha competent *E. coli* cells according to the supplier's protocol. Briefly, *E. coli* cells were thawed on ice for 10 minutes and 1-5 µl of plasmid DNA was added. Cells were incubated for 30 min on ice and were then heat shocked at 42°C for 30 seconds. Cells were then placed on ice for 5 minutes. Cells were serially diluted using LB and plated on LB + ampicillin (100 µg/ml) at 30°C for 24 hours. Plasmids were isolated from *E. coli* using the Geneaid High Speed Plasmid Mini-Kit according to the supplier's protocol.

2.7.1 Creation of the pJK210-*adn2*-GFP construct

The pJK210-*adn2*-GFP construct was created using PCR-based cloning. The carboxy terminus of the *adn2* gene was amplified by PCR from wild-type genomic DNA using the following primers (forward: 5'-GGGGGAATTCTGACCTGATAGACCGCTTTCTCAG-3'; reverse: 5'-GGGGCCCCGGGAGCAGCAGTCGAGTCTTCATT-3'). The amplicon was then cloned in frame and upstream of the GFP gene using the *EcoRI* and *XmaI* sites present

in the pJK210-GFP plasmid. The plasmid was then transformed into wild-type strain, JK484, using the lithium acetate method (Forsburg and Rhind, 2006). The transformed cells were selected by growth on EMM solid media lacking uracil. The transformant cells were further verified for locus specific homologous recombination by colony PCR using the following primers (forward: 5'-CCTAACCTGCTCAACAGCC-3'; reverse: 5'-TGGGACAACCTCCAGTGAAAA-3').

2.7.2 Creation of the pREP1-*adn2*, pREP41-*adn2* and pREP81-*adn2* over-expression constructs

The full length *adn2* gene was PCR amplified from wild-type genomic DNA using primers flanked by *XmaI* and *NdeI* sites (forward: 5'-GGCGGCATATGGCTGATCCAGGTTTAAGGT-3'; reverse: 5'-GGCGGCCCGGGTTAAGCAGCAGTCGAGTCTTCATTA-3'). Both the pREP series of vectors and the PCR amplicon were digested using *XmaI* and *NdeI* restriction enzymes by incubating for 1 hour at 37°C. The plasmid and amplicon digests were run and purified from a 1% agarose gel. The *adn2* gene was then ligated to the digested pREP series of plasmids using the New England Biolabs Quick Ligation kit according to the supplier's protocol.

2.8 Live cell imaging

Rlc1-GFP expressed from the native *rlc1* promoter was used as a marker to monitor actomyosin ring constriction in live cells. Cells were cultured in liquid YES to mid-log phase at 30°C and then treated with 0.2 µM LatA or DMSO (solvent control). Cells were then visualized under the GFP filter set by time-lapse fluorescence microscopy using a LEICA DMI6000B inverted fluorescence microscope.

2.9 *adn2* over-expression analysis

The pREP1-*adn2*, pREP41-*adn2*, and pREP81-*adn2* plasmids were transformed into wild-type *S. pombe* cells using the lithium acetate method (Forsburg and Rhind, 2006) and Leu⁺ transformants isolated. Strains containing the respective constructs were then cultured in EMM supplemented with thiamine (10 μ M) and lacking leucine to mid-log phase. 1 mL of each culture was then used to inoculate fresh liquid EMM containing thiamine (+T) or lacking thiamine (-T). Cells were grown for a further 18 hours and treated with DMSO or 0.1 μ M, 0.2 μ M or 0.3 μ M of LatA. Cells were then cultured for a further 5 hours before being fixed with ethanol and stained with DAPI/aniline blue. Cells were imaged as described in Section 2.6.

Chapter 3

3 Results

3.1 Primary screen

When challenged with low doses of LatA (0.2 - 0.5 μ M), fission yeast mutants defective in the cytokinesis checkpoint system exhibit a terminal phenotype characterized by inviable multi-nucleate cells that have failed in cytokinesis. In contrast, wild-type cells remain viable under these same conditions and are able to complete cytokinesis, albeit over a longer time-frame than normal (Mishra et al. 2004; Mishra et al. 2005; Chen et al. 2005; Karagiannis et al. 2005; Karagiannis and Balasubramanian, 2007; Saberianfar et al. 2011; Rentas et al., 2012). It was thus reasoned that this characteristic LatA sensitive phenotype could be used as the basis of a screen aimed at identifying novel genes with roles in promoting successful cell division upon perturbation of the cytokinetic machinery. It was also reasoned that the screen would prove useful in identifying genes with roles in adapting to LatA induced cytoskeletal stress in general. Version 4 of the Bioneer gene deletion library (Kim et al., 2010) was thus obtained and used to carry out a screen for deletion mutants exhibiting hypersensitivity to LatA. A schematic providing a broad overview of the screen described in this thesis is shown in **Figure 3-1**.

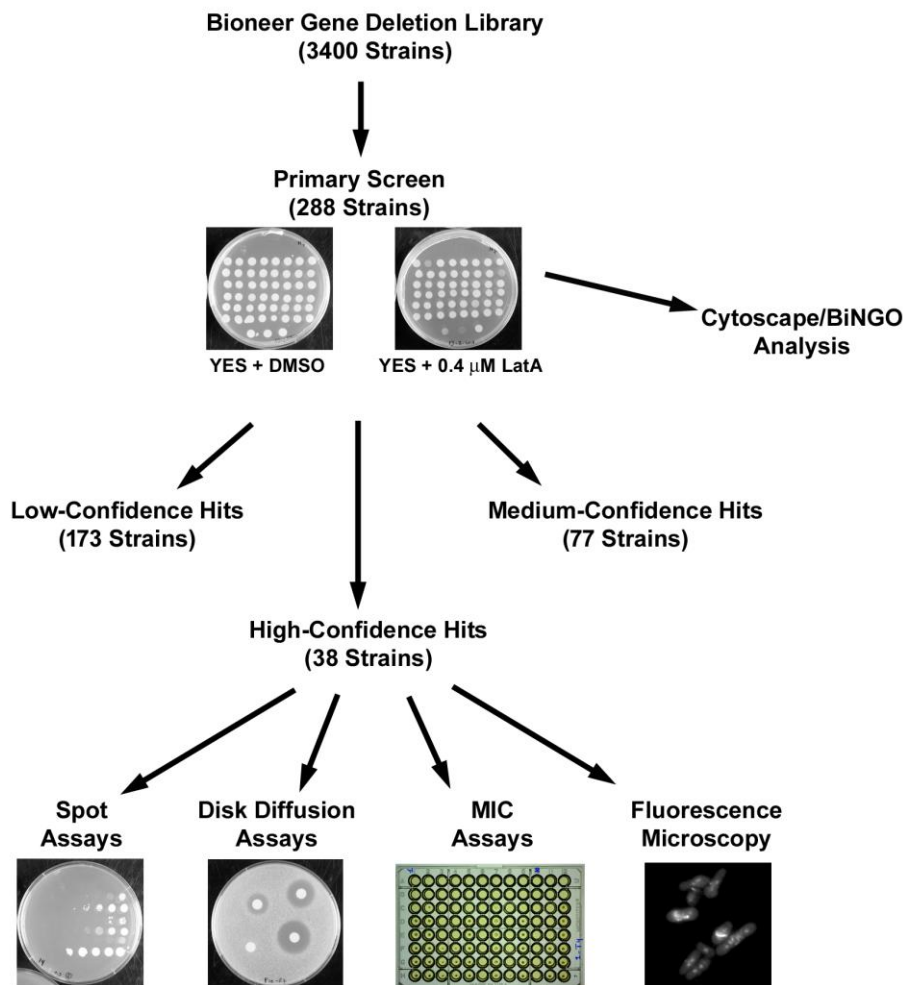


Figure 3-1 Overview of the genetic screen described in this thesis. A total of 3400 strains derived from the Bioneer fission yeast gene deletion mutant library were screened on YES-agar media containing DMSO (solvent control) or 0.4 μM LatA. A total of 38 strains were scored as hits in all three trials (high-confidence group), 77 strains were scored as hits in two of three trials (medium-confidence group), and 173 strains were scored as hits in one of three trials (low-confidence group). The high-confidence hits were further validated and analyzed by spot assays, disk diffusion assays, minimum inhibitory concentration (MIC) assays, and by fluorescence microscopy.

The entire library of 3400 strains was screened by plating the gene deletion mutants on YES medium containing 0.4 μ M LatA and incubating them for 3 days at 30°C (see Materials and Methods). Growth was compared to the same mutants plated on YES medium containing DMSO (solvent control). To minimize false negatives, the primary screen was performed in triplicate. Three strains were used as controls: *lsk1Δ*, a known LatA sensitive mutant showing low to moderate sensitivity (Karagiannis et al., 2005), *pap1Δ*, a mutant known to be hypersensitive to a wide variety of toxins (and which we observed to be highly sensitive to LatA; J. Karagiannis and B. Chakraborty, unpublished), and lastly, a wild-type strain. Representative plates from one trial of the screen are shown in **Figure 3-2A**.

After completing the primary screen, we categorized the hits into three groups: a “high-confidence” group of 38 strains, a “medium-confidence” group of 77 strains, and a “low-confidence” group of 173 strains (**Figure 3-2B; Appendix A**). The “high-confidence” group comprised of gene deletion mutants that were scored as hits in each of the three trials. The “medium-confidence” group comprised gene deletion mutants that were scored as hits in two of the three trials. Finally, the “low-confidence” group comprised gene deletion mutants that were scored as hits in only one of the three trials. Of eight previously characterized LatA sensitive mutants present in version 4 of the library, two were present in the low confidence group (*lsk1Δ*, *hos2Δ*), and six were present in the medium-confidence group (*clp1Δ*, *rad24Δ*, *lsg1Δ*, *sif2Δ*, *snt1Δ*, *set3Δ*).

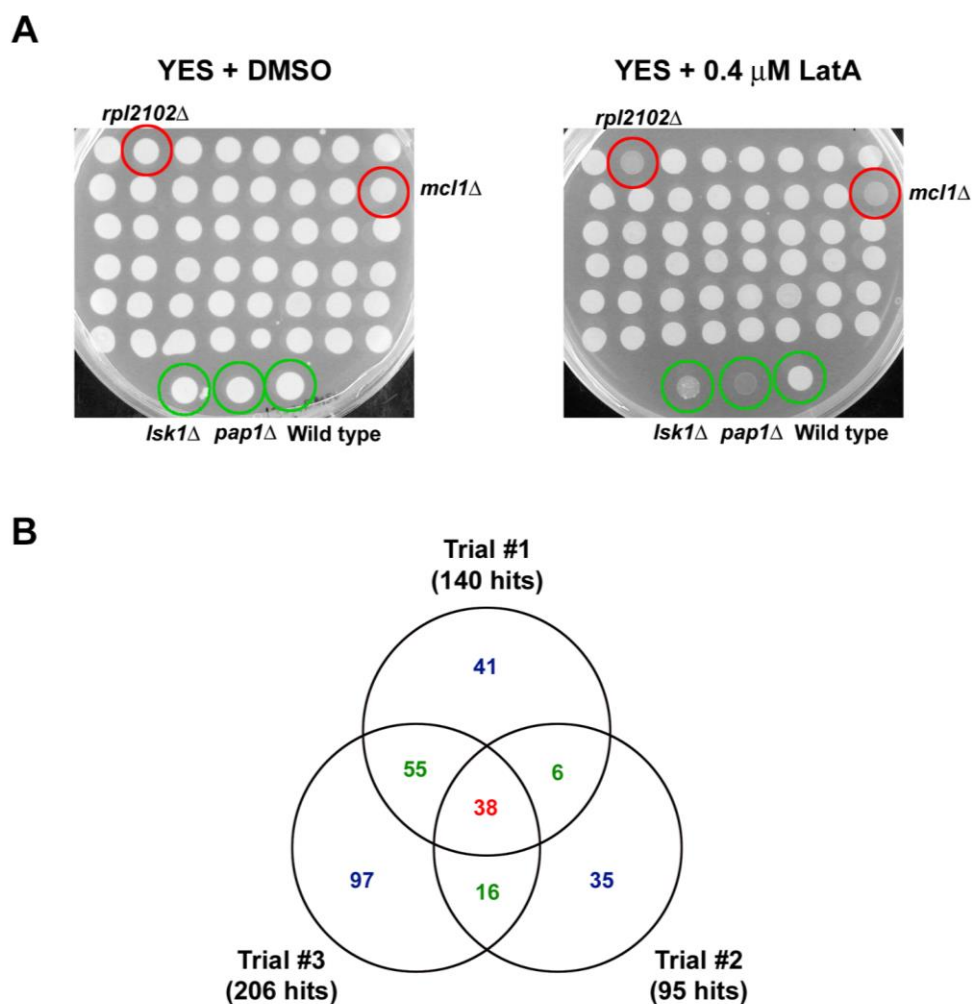


Figure 3-2 Primary screen. (A) All 3400 gene deletion strains from the Bioneer collection were spotted to YES-agar plates containing DMSO (solvent control) or 0.4 μ M LatA and then incubated for 3 days at 30°C. Two representative plates from the screen are shown. A wild-type strain, as well as two hyper-sensitive mutants, *lsk1* Δ , and *pap1* Δ , were used as controls (green circles). Two “hits”, *rpl2102* and *mcl1* Δ are also highlighted (red circles). (B) Venn diagram analysis of the three trials of the primary screen. Thirty-eight hits were common to all three trials and comprise the high-confidence group (red). Seventy-seven hits were common to two of the trials and comprise the medium-confidence group (green). One hundred and seventy-three hits were common to one of the three trials and comprise the low-confidence group (blue).

While the low-confidence group is likely high in false positives, I include the data here for the sake of completeness. Moreover, the fact that both *lsk1Δ* and *hos2Δ* were categorized as low-confidence hits suggests that the group contains at least some true positives. In contrast, the high- and medium-confidence lists, while lower in false positives, must by the same token suffer from higher false negative rates. Thus, by including the complete primary data set in its entirety (high-, medium-, and low-confidence lists), I strike the best balance with respect to mitigating the effects of false negative and false positive categorizations and provide the broadest resource possible.

3.2 Secondary screening

Having completed the primary screen, I focused on the deletion mutants of the high confidence group for the remainder of the study. Ten-fold serial dilutions of logarithmically growing cultures of each of the high confidence hits were spotted onto YES medium containing DMSO or 0.1 μM , 0.2 μM , or 0.3 μM LatA. These experiments verified that the mutants were indeed hyper-sensitive to LatA (**Figure 3-3**). The sensitivity of the mutants varied from mild (capable of moderate growth on 0.3 μM LatA relative to wild-type) to severe (incapable of growth even at 0.1 μM LatA).

To provide a more quantitative assessment of LatA sensitivity, a series of disk diffusion assays were performed (see Materials and Methods). In these assays filter paper disks soaked in DMSO (solvent control), or 2.2 μM , 4.4 μM , or 6.6 μM LatA, were placed on YES agar plates impregnated with the respective gene deletion mutants. The plates were then incubated at 30°C for four days. Representative plates (*pap1Δ* and wild-type controls, as well as three gene deletion mutants displaying varying levels of sensitivity) are shown in **Figure 3-4A**.

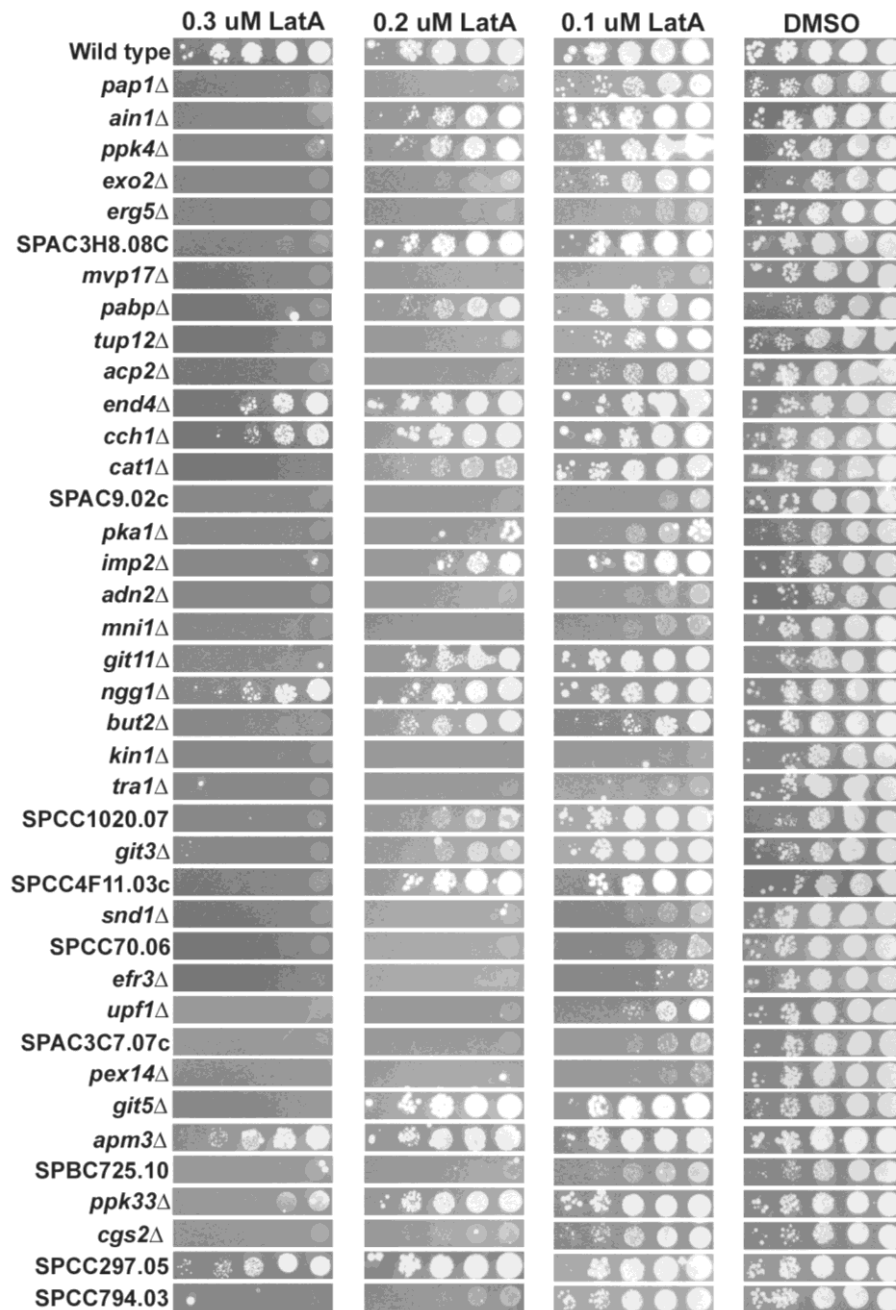


Figure 3-3 Spot assays. Ten-fold serial dilution of cultures of the indicated genotypes were spotted onto YES-agar plates containing DMSO (solvent control), or 0.1 μ M, 0.2 μ M, or 0.3 μ M LatA. Photographs were taken after four days incubation at 30°C.

For each strain, the area of the zone of inhibition around each disk was plotted against LatA concentration. Linear regression was then used to create a line of best fit through the data points. The slopes of the lines were then calculated. Using this quantitative measure it was possible both to validate the high confidence hits, as well as accurately rank the strains according to their sensitivity to LatA (**Figure 3-4B, Table 3-1**).

Lastly, the mutants' sensitivity to LatA was gauged by determining the minimum inhibitory concentration (MIC) for each of the high confidence hits. This was accomplished using the method of Tebbets et al. (2012). Briefly, 10^5 cells of an overnight culture of each mutant were seeded into the wells of a microtiter plate. Each well contained 100 μL of YES media containing LatA at concentrations ranging from 0.025 to 0.2 μM . The plates were then incubated at 30°C for four days. The MIC was defined as the lowest concentration of LatA that prevented visible growth. The MICs varied from $>0.2 \mu\text{M}$ for wild-type cells to 0.025 μM for the most sensitive mutants (**Table 3-2**).

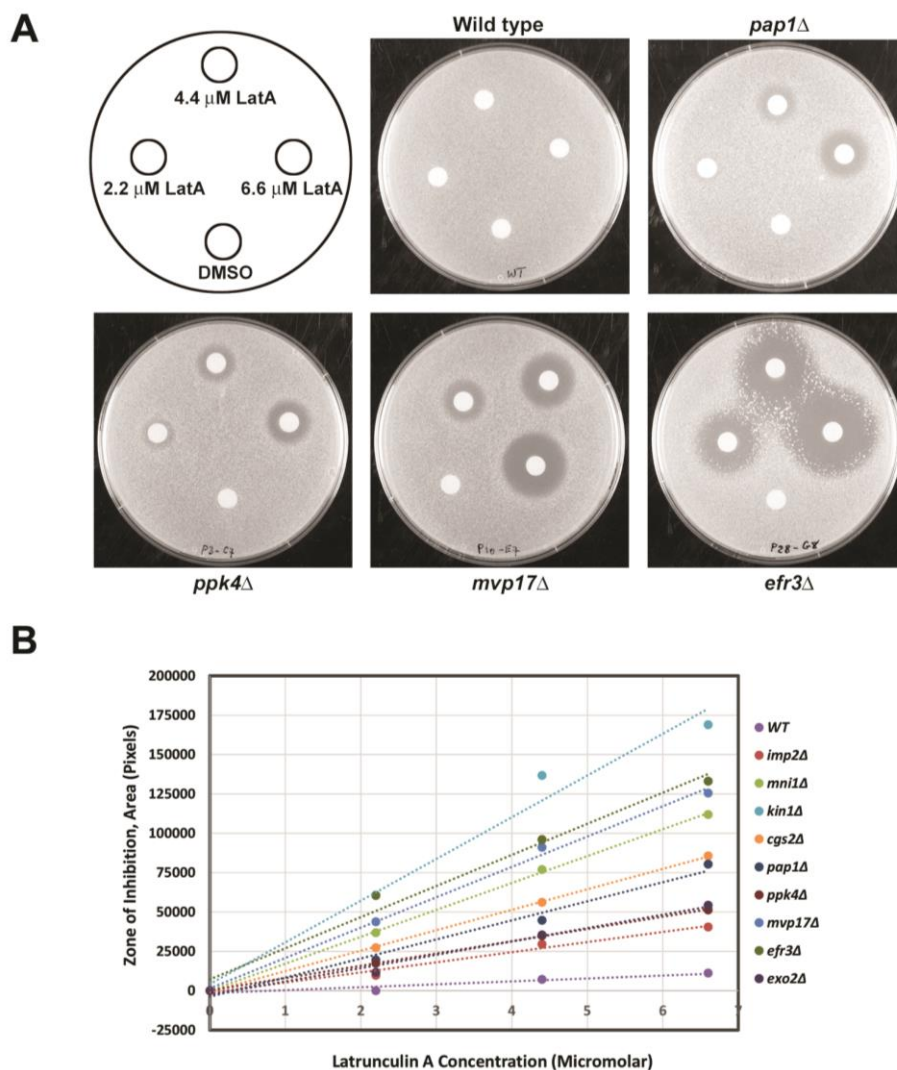


Figure 3-4 Disk diffusion assays. (A) Filter paper disks soaked with 5 μ L of DMSO (solvent control) or 2.2 μ M, 4.4 μ M, or 6.6 μ M LatA, were placed on YES-agar plates impregnated with the indicated gene deletion mutants. Photographs were taken after four days incubation at 30°C. The zones of growth inhibition surrounding each disk were measured and analyzed as described in the Materials and Methods. (B) A plot of the area of the zone of inhibition vs. LatA concentration for a representative group of 10 gene deletion strains exhibiting varying sensitivity to LatA. The linear regression line through the points is plotted. The slope of this line was used as a quantitative measure to rank the LatA sensitivity of each strain.

Table 3-1 Ranking of the LatA sensitivity of each gene deletion mutant based on linear regression analysis of data plotting the area of the zone of inhibition (pixels) vs. LatA concentration (μM).

Gene Deletion	Rank (Most Sensitive to Least Sensitive)	Slope of the Linear Regression Line (pixels/ μM)
<i>kin1Δ</i>	1	26505
<i>cch1Δ</i>	2	22989
<i>efr3Δ</i>	3	19765
<i>adn2Δ</i>	4	19447
<i>mvp17Δ</i>	5	19283
<i>pex14Δ</i>	6	17437
<i>pka1Δ</i>	7	17303
<i>mni1Δ</i>	8	17085
<i>acp2Δ</i>	9	16543
SPCC794.03	10	16403
SPCC70.06	11	16360
SPAC9.02c	12	15836
<i>erg5Δ</i>	13	15748
<i>tra1Δ</i>	14	15388
<i>snd1Δ</i>	15	15216
SPAC3C7.07c	16	14287
<i>upf1 Δ</i>	17	13785
SPCC297.05	18	12995
<i>pap1Δ</i>	19	12108
<i>pabpΔ</i>	20	10286
<i>tup12Δ</i>	21	9763
SPCC4F11.03c	22	9749
<i>ngg1Δ</i>	23	9289
<i>git5Δ</i>	24	8890
<i>ain1Δ</i>	25	8717
<i>exo2Δ</i>	26	8480
<i>cat1Δ</i>	27	8312
<i>git3Δ</i>	28	8062
<i>ppk4Δ</i>	29	7802
SPBC725.10	30	7485
SPCC1020.07	31	7064
<i>git11Δ</i>	32	6670
<i>ppk33Δ</i>	33	6669
<i>imp2Δ</i>	34	6424
<i>apm3Δ</i>	35	5886
SPAC3H8.08c	36	5555
<i>end4Δ</i>	37	4862
<i>but2Δ</i>	38	4711
<i>cgs2Δ</i>	39	4080
Wild type	40	1852

Table 3-2 Minimum inhibitory concentration of LatA for the indicated gene deletion mutants.

Gene Deletion Mutant	Minimum Inhibitory Concentration (μM)
<i>ain1</i> Δ	0.1-0.2
<i>ppk4</i> Δ	.2
<i>exo2</i> Δ	0.075
<i>erg5</i> Δ	0.025-0.075
SPAC3H8.08c	0.2
<i>mvp17</i> Δ	.05
<i>pabp</i> Δ	0.1-0.2
<i>tup12</i> Δ	0.025
<i>acp2</i> Δ	0.1-0.2
<i>end4</i> Δ	0.2
<i>cch1</i> Δ	>0.2
<i>cat1</i> Δ	0.1-0.2
SPAC9.02c	0.075-0.1
<i>pka1</i> Δ	0.2
<i>imp2</i> Δ	0.025
<i>adn2</i> Δ	0.025
<i>mni1</i> Δ	0.05
<i>git11</i> Δ	0.2
<i>ngg1</i> Δ	0.2
<i>but2</i> Δ	0.2
<i>kin1</i> Δ	0.025
<i>tra1</i> Δ	0.05
SPCC1020.07	0.2
<i>git3</i> Δ	0.1-0.2
SPCC4F11.03c	0.1
<i>snd1</i> Δ	0.075-0.1
SPCC70.06	0.075
<i>efr3</i> Δ	0.05-0.075
<i>upf1</i> Δ	0.075-0.1
SPAC3C7.07c	0.075-0.1
<i>pex14</i> Δ	0.05-0.075
<i>git5</i> Δ	0.2
<i>apm3</i> Δ	>0.2
SPBC725.10	0.1-0.2
<i>ppk33</i> Δ	0.2
<i>cgs2</i> Δ	0.075
SPCC297.05	>0.2
SPCC794.03	0.05
<i>pap1</i> Δ	0.05-0.075
Wild type	>0.2

3.3 Screening for cytokinesis mutants

Having validated the high-confidence hits, it was important next to characterize the nature of each mutant's sensitivity to LatA. To screen for any obvious cytokinetic phenotypes, the respective mutants were treated with 0.3 μ M LatA for 5 hours. The cell nuclei as well as cell wall/septal material were then visualized by fixing the cells and staining with a mixture of DAPI and aniline blue. The cells were then classified into one of four categories: 1) uninucleate cells, 2) bi-nucleate cells with complete septa, 3) bi-nucleate cells with fragmented/incomplete septa, and 4) tetra-nucleate cells with fragmented/incomplete septa. We then calculated the ratio of binucleate or tetranucleate cells with fragmented/incomplete septa, to uninucleate cells or binucleate cells with complete septa.

While the wild-type control strain accumulated a majority of cells that were uninucleate, or binucleate with complete septa, the 38 mutants of the high confidence group accumulated much higher proportions of cells with fragmented/incomplete septa (indicating failed constriction of the actomyosin ring) (**Figure 3-5, Table 3-3**). In fact, 15 of the 38 mutants (39%) exhibited a majority of cells with fragmented septa. Importantly, although compromised in their ability to complete cytokinesis in the presence of LatA, the high-confidence mutants were nevertheless fully capable of successful cell division in the presence of DMSO. The mutants of the high confidence group are thus defective in some aspect of their response to LatA-induced cytoskeletal perturbation and are thereby more prone to cell division failure. The mechanism(s) underlying the observed cytokinetic defects of the high confidence mutants are unknown and will be the subject of future studies.

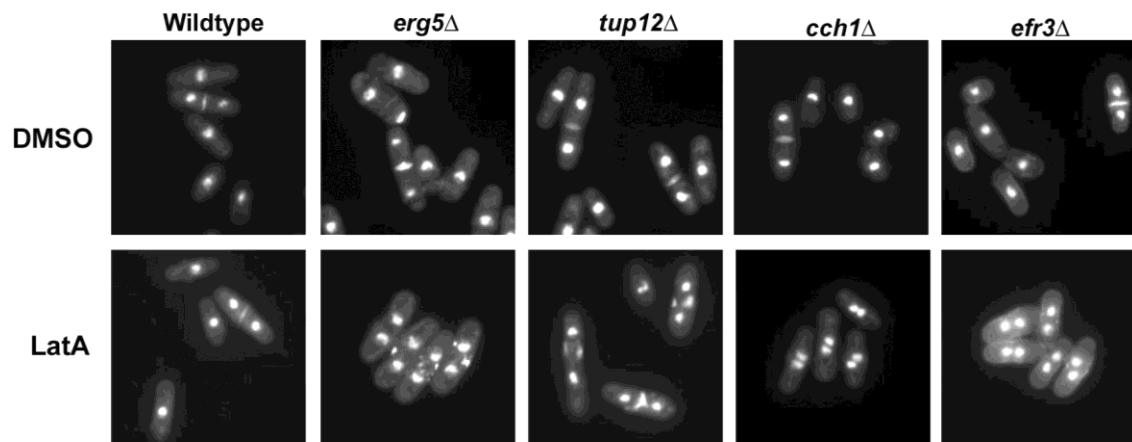


Figure 3-5 The gene deletion mutants of the high-confidence list are prone to cytokinesis failure in the presence of LatA. Cells of the indicated genotype were grown to mid-log phase and then treated with DMSO (solvent control) or 0.3 μ M LatA for 5 hours. Cells were fixed and stained with DAPI/aniline blue to visualize nuclei and cell/wall septal material, respectively. Four strains from the high-confidence list are shown as representative examples.

Table 3-3 Mean percentage of cells (+/- SD) displaying the indicated phenotype after 5 hours treatment with 0.3 μ M Latrunculin A (n=3).

Gene Deletion Mutant	Uninucleate	Binucleate (Complete Septum)	Binucleate (Fragmented Septum)	Tetranucleate (Fragmented Septum)	Ratio (Fragmented/Non-fragmented)
<i>ain1</i> Δ	69 +/- 14	3 +/- 3	28 +/- 15	0	0.39
<i>ppk4</i> Δ	44 +/- 29	1 +/- 1	52 +/- 27	4 +/- 6	1.16
<i>exo2</i> Δ	21 +/- 12	2 +/- 2	76 +/- 11	1 +/- 2	3.30
<i>erg5</i> Δ	53 +/- 36	2 +/- 3	43 +/- 37	1 +/- 1	0.78
SPAC3H8.08c	68 +/- 18	5 +/- 7	27 +/- 11	0	0.36
<i>mvp17</i> Δ	19 +/- 14	7 +/- 6	70 +/- 9	4 +/- 3	2.66
<i>pabp</i> Δ	23 +/- 5	0	72 +/- 4	4 +/- 1	3.10
<i>tup12</i> Δ	43 +/- 31	3 +/- 5	54 +/- 35	1 +/- 1	1.18
<i>acp2</i> Δ	66 +/- 20	1 +/- 1	33 +/- 20	0	0.50
<i>end4</i> Δ	60 +/- 19	1 +/- 1	34 +/- 14	1 +/- 2	0.56
<i>cch1</i> Δ	41 +/- 31	2 +/- 2	56 +/- 31	0	1.30
<i>cat1</i> Δ	51 +/- 18	3 +/- 6	43 +/- 14	2 +/- 3	0.79
SPAC9.02c	46 +/- 27	5 +/- 6	47 +/- 34	0	0.92
<i>pka1</i> Δ	62 +/- 14	3 +/- 4	32 +/- 9	2 +/- 3	0.48
<i>imp2</i> Δ	10 +/- 5	0	69 +/- 2	21 +/- 5	7.14
<i>adh2</i> Δ	24 +/- 20	1 +/- 2	72 +/- 19	3 +/- 3	2.83
<i>mni1</i> Δ	65 +/- 11	7 +/- 3	28 +/- 7	0	0.39
<i>git11</i> Δ	54 +/- 19	1 +/- 2	44 +/- 21	0	0.81
<i>ngg1</i> Δ	22 +/- 4	2 +/- 3	75 +/- 6	1 +/- 1	3.14
<i>but2</i> Δ	63 +/- 9	2 +/- 3	34 +/- 6	0	0.52
<i>kin1</i> Δ	18 +/- 5	11 +/- 9	63 +/- 14	8 +/- 2	2.16
<i>tra1</i> Δ	47 +/- 12	8 +/- 7	43 +/- 12	2 +/- 2	0.79
SPCC1020.07	47 +/- 32	3 +/- 1	49 +/- 30	1 +/- 1	0.99
<i>git3</i> Δ	53 +/- 21	0 +/- 0	45 +/- 21	2 +/- 2	0.84
SPCC4F11.03c	31 +/- 14	6 +/- 9	58 +/- 21	5 +/- 2	1.54
<i>snd1</i> Δ	39 +/- 12	5 +/- 6	55 +/- 17	1 +/- 1	1.26
SPCC70.06	41 +/- 20	5 +/- 5	52 +/- 26	2 +/- 2	1.12
<i>efr3</i> Δ	32 +/- 17	2 +/- 2	66 +/- 18	0	1.91
<i>upf1</i> Δ	39 +/- 27	3 +/- 3	58 +/- 29	1 +/- 1	1.38
SPAC3C7.07c	54 +/- 10	9 +/- 2	35 +/- 12	2 +/- 3	0.56
<i>pex14</i> Δ	70 +/- 8	8 +/- 8	22 +/- 5	0	0.28
<i>git5</i> Δ	55 +/- 16	2 +/- 2	42 +/- 19	2 +/- 3	0.74
<i>apm3</i> Δ	48 +/- 5	3 +/- 1	48 +/- 3	1 +/- 1	0.94
SPBC725.10	53 +/- 24	1 +/- 2	45 +/- 23	0	0.82
<i>ppk33</i> Δ	58 +/- 8	5 +/- 5	37 +/- 3	0	0.60
<i>cgs2</i> Δ	60 +/- 4	4 +/- 4	36 +/- 6	0	0.56
SPCC297.05	59 +/- 27	2 +/- 3	38 +/- 28	0	0.63
SPCC794.03	60 +/- 16	7 +/- 6	31 +/- 14	1 +/- 2	0.47
<i>pap1</i> Δ	46 +/- 11	1 +/- 1	53 +/- 11	0	1.14
Wild type	88 +/- 3	12 +/- 3	2 +/- 1	0	0.02

3.4 Bioinformatical analysis of the *adn2* gene

The ultimate goal of the project described in this thesis was to understand the molecular mechanisms by which the identified genes mitigate the detrimental effects of abnormal cytoskeletal perturbations. Since a detailed characterization of all of the hits would be well beyond the scope of a single MSc project, I decided to focus my attention on a single gene. Due to my interest in transcriptional mechanisms, I chose the most highly ranked transcription factor from the high-confidence list of hits. The gene is referred to as *adn2* (for adhesion defective).

adn2 was first identified in a functional genomic screen for genes involved in adhesion, invasion, and mycelial formation (Dodgson et al., 2009). This study identified 12 genes required for mycelial development. Of these 12 genes, two (including *adn2*) were defective in the initial adhesion of the cells to the surface of the growth medium (this represents the first stage of mycelial formation). Little else is known with respect to the function of the *adn2* gene. To begin my analysis of the functional roles of the encoded gene-product, I made use of available bioinformatical tools to learn more with respect to its domain structure, its evolutionary relatedness to other proteins, and its protein interaction network. These analyses are described below.

3.4.1 Domain structure

The Adn2p protein sequence was obtained from Pombase (www.pombase.org/) and input into the Simple Modular Architecture Research Tool (<http://smart.embl-heidelberg.de/>) with the PFAM domain search box checked. This search identified i) a

LisH domain, ii) a single stranded DNA binding domain, and iii) two coiled-coil domains (**Figure 3-6**).

The LisH motif is found in eukaryotic proteins involved in microtubule dynamics, cell migration, and chromosome segregation. It is thought that the LisH domain contributes to the regulation of microtubule dynamics. SSDP defines a single-stranded DNA binding domain with specificity to pyrimidine-rich elements found in the promoter regions of target genes. Coiled-coils are alpha-helical structures that mediate subunit oligomerization of a variety of different proteins, including transcription factors. The above analysis thus implicated Adn2p in both the regulation of the microtubule cytoskeleton, and in the regulation of transcription.

3.4.2 Phylogenetic analysis

To determine whether Adn2p defines a conserved family of proteins, the DRSC Integrative Ortholog Prediction Tool(www.flyrnai.org/cgi-bin/DRSC_orthologs.pl) was used to identify related proteins. This analysis revealed that Adn2p was part of a family of 17 related genes (bearing SSDP domains) present in budding yeast, *Drosophila*, mouse, rat, *C. elegans*, zebrafish and humans. The individual protein sequences were then obtained and input into the phylogeny.fr phylogeny analysis tool (www.phylogeny.fr/simple_phylogeny.cgi). This tool uses the MUSCLE algorithm for multiple alignment, the PHYML algorithm for phylogenetic analysis, and the TreeDyn algorithm for tree rendering. The results of this analysis are shown in **Figure 3-7**.

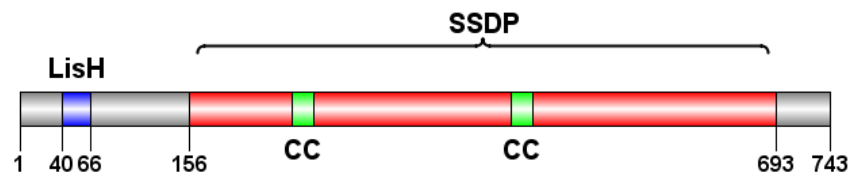


Figure 3-6 Domain Structure of Adn2p. LisH, Lissencephaly type-1-like homology motif; SSDP, single stranded DNA binding protein; CC, coiled coil.

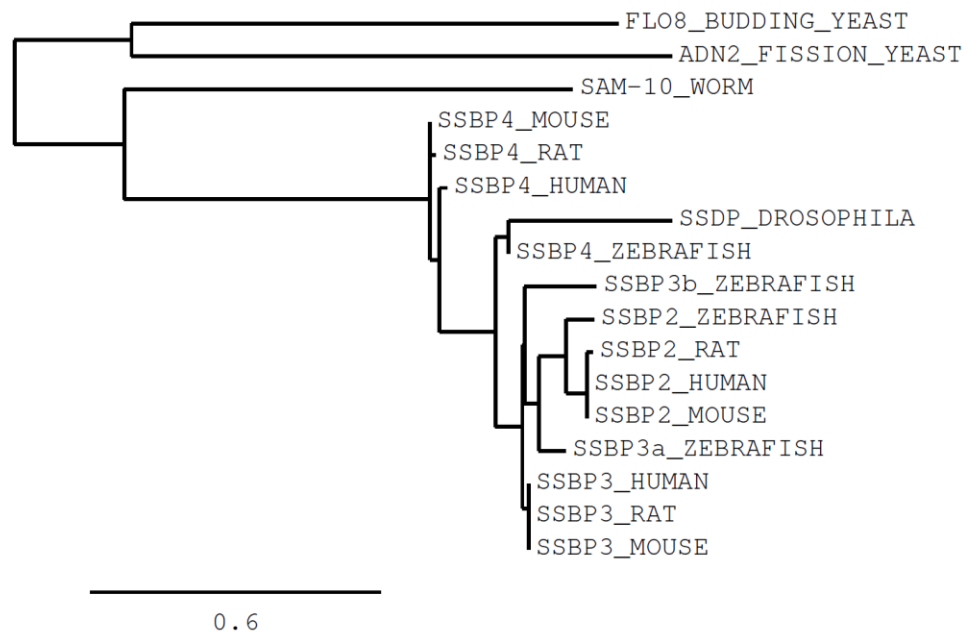


Figure 3-7 Phylogenetic analysis of Adn2p and its related proteins. The MUSCLE algorithm was used for multiple alignment, the PHYML algorithm for phylogenetic analysis, and the TreeDyn algorithm for tree rendering. Scale bar, 0.6 amino acid substitutions per site. Protein sequences were obtained from the NCBI database. Bootstrap value =1000.

This analysis revealed that the closest ortholog of Adn2p was the budding yeast, FLO8 protein, but that significant sequence divergence had occurred over evolutionary time. Similarity between Adn2p and its metazoan orthologs is restricted to the SSDP domain. With the exception of FLO8 (required for flocculation), and SAM-10 (required for presynaptic differentiation and neurite branching) little is known with respect to the biological functions of the related proteins (Kim et al., 2014; Zheng et al., 2011).

3.4.3 Protein interaction network

To explore the protein interaction network surrounding Adn2p, the BioGrid database (thebiogrid.org/) was queried to identify Adn2p binding partners. This analysis revealed a small interactome of only three proteins, the alpha-importin, Imp1p, the phosphatidylinositol-3-phosphate binding protein, SPAC6F6.12, and the uncharacterized, SPBC354.04 (**Figure 3-8**). Interestingly, two of the three interactors (*imp1* and SPAC6F6.12) were also identified as hits in our original screen for LatA sensitive mutants. Thus, Adn2p might be part of a multi-protein complex with roles in defending against cytoskeletal perturbations (see Discussion).

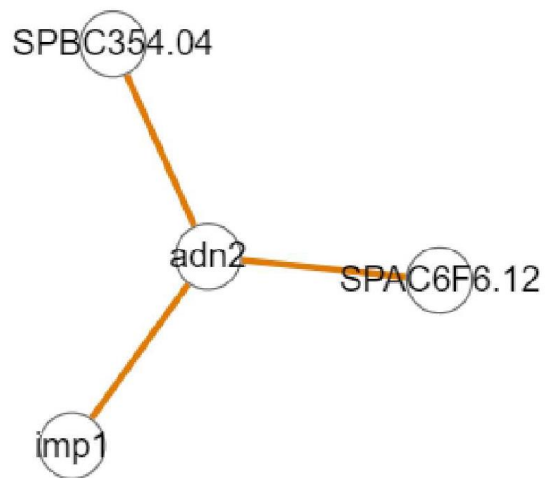


Figure 3-8 Protein interaction network of the Adn2p protein. Interaction data was obtained from the BioGrid database (thebiogrid.org/). The network was visualized using EsyN (www.esyn.org).

3.5 Live-cell imaging of cytokinesis in *adn2Δ* mutants

To obtain more detailed information (in real-time) as to the effects of *adn2* loss of function mutations on the process of cytokinesis in *S. pombe*, I imaged *adn2Δ* strains expressing the Rlc1-GFP fusion protein. *rlc1* encodes for the myosin II regulatory light chain and thus serves as an excellent marker for visualizing constriction of the actomyosin ring.

I began by examining actomyosin ring constriction in the absence of LatA in both an *adn2Δ* strain and a wild-type control. In the presence of DMSO (solvent control), both the wild-type strain (**Figure 3-9A**) and the *adn2Δ* strain (**Figure 3-9B**) were able to successfully complete cytokinesis within 30-35 minutes. When treated with 0.2 μ M LatA, the wild-type strain was able to constrict the actomyosin ring, however, where it took approximately 30-35 minutes under control conditions, it took about 70 minutes for cells to complete cytokinesis in the presence of LatA (**Figure 3-9C**). This is due to the cell being held in a prolonged cytokinesis competent state, characterized by continuous repair/reestablishment of the actomyosin ring.

When treated with 0.2 μ M LatA the *adn2Δ* strain was unable to successfully constrict the actomyosin ring (**Figure 3-9D**). While the actomyosin ring was able to form, GFP expression became progressively weaker over time and the ring was eventually lost (without constricting) after 30-35 minutes. This suggests that Adn2p, while not required for ring assembly, is essential for proper ring maintenance and constriction upon perturbation of the cytokinetic machinery in response to LatA induced stress.

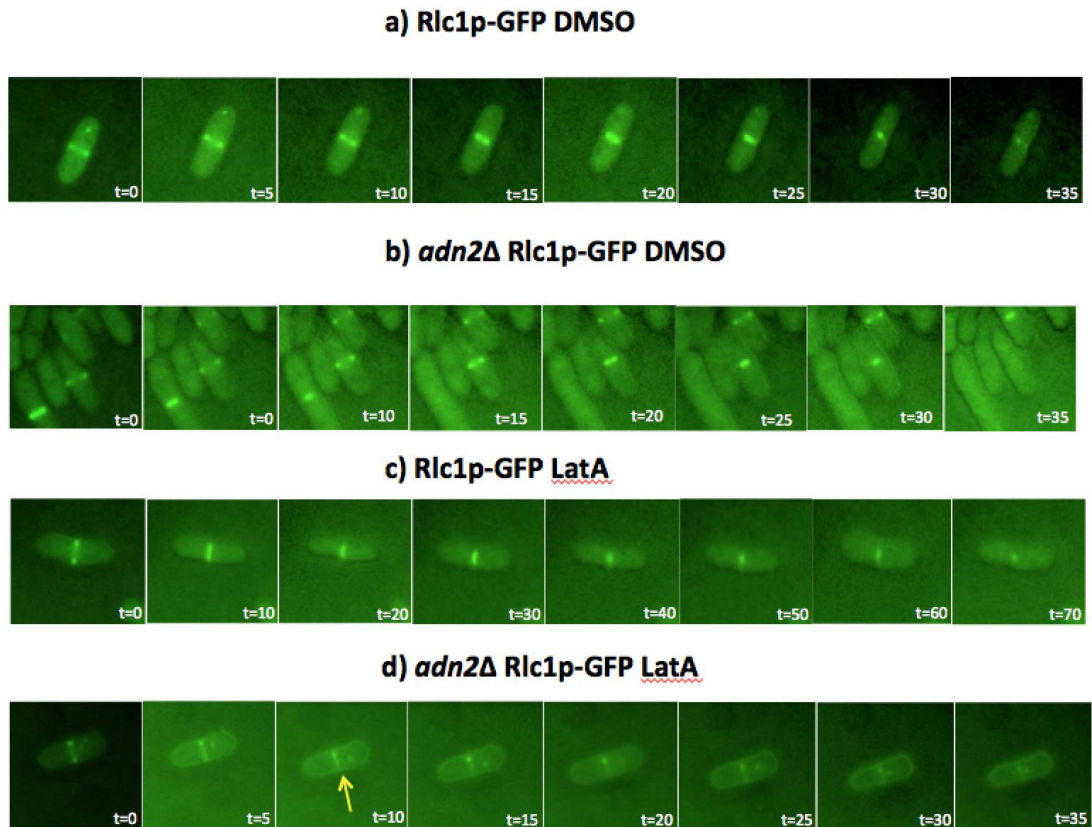


Figure 3-9 *adn2Δ* mutants are unable to constrict the actomyosin ring when treated with LatA. Wild-type and *adn2Δ* cells expressing Rlc1p-GFP were grown overnight to mid-log phase in YES media. The strains were then imaged in real time by fluorescence microscopy using the GFP filter. **A)** Wild-type cells treated with DMSO. **B)** *adn2Δ* cells treated with DMSO. **C)** Wild-type cells treated with 0.2 Mm LatA. **D)** *adn2Δ* cells treated with 0.2 μ M LatA. Time in minutes is indicated at the bottom right of each image.

3.6 Over-expression analysis of the *adn2* gene

Up to this point, my studies had clearly shown that the loss of *adn2* results in cytokinetic defects when cells are challenged with LatA. To determine the effects of Adn2p over-expression I created three different expression constructs (pREP1-*adn2*, pREP41-*adn2*, and pREP81-*adn2*) in which *adn2* was under the respective control of one of three thiamine repressible *nmt* promoters: *nmt1* (strong overexpression), *nmt41* (moderate overexpression) and *nmt81* (low overexpression) (Basi et., 1993). The over-expression strains were grown in liquid EMM medium in both the presence or absence of thiamine, to mid-log phase. Cells from each culture were then treated with DMSO or 0.1 μ M, 0.2 μ M, or 0.3 μ M LatA, and grown for a further 5 hours. Cells were then fixed with ethanol, stained with DAPI/aniline blue, and visualized using fluorescence microscopy (**Figure 3-10**).

Interestingly, strains with the highest level of Adn2p overexpression (pREP1-*adn2*) grown in the absence of thiamine showed phenotypic abnormalities that included fragmented septa, tetranucleate cells and multiple septa (**Figure 3-10**, arrows). In contrast, strains with low/moderate levels of Adn2p overexpression (grown either in the presence or absence of thiamine) did not show any of these cellular phenotypes. These data suggest that Adn2p overexpression has a dominant negative effect leading to cytokinetic abnormalities (see Discussion).

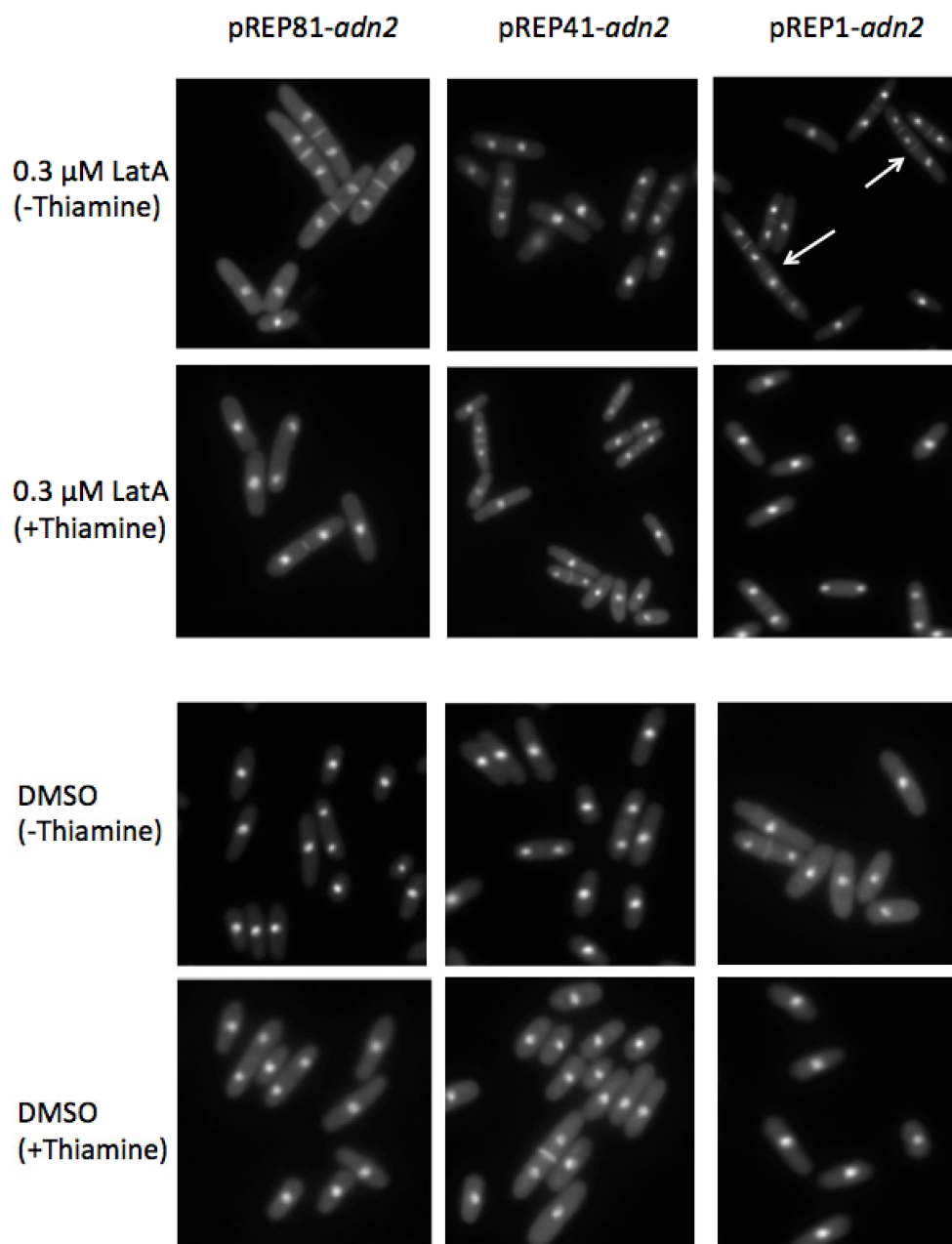


Figure 3-10: Cell nucleus and wall/septum staining of strains over-expressing *adn2*. Adn2p overexpression plasmids were treated with 0.3 μ M LatA or DMSO for 5 hours. Overexpression was repressed by adding thiamine to LatA and DMSO cultures, to act as repressed controls. To visualize the cell nucleus and wall/septum, cells were stained with DAPI (nucleus) and aniline blue (wall/septum). Cells were visualized with fluorescence microscopy using a DAPI filter. Arrows point to cells with multiple septa.

3.7 Intracellular localization of Adn2-GFP

The intracellular localization of a protein often reveals clues as to its functional role within the cell. To assess the localization of Adn2p, I constructed a vector containing the carboxy terminus of *adn2* fused in-frame with the GFP coding sequence (see Materials and Methods). This construct was then homologously integrated at the *adn2* locus creating a strain expressing full length Adn2-GFP fusion proteins under the control of the native *adn2* promoter.

To assess the localization of Adn2p under normal growth conditions, strains were grown to mid-log phase in YES medium and then observed by live-cell fluorescence microscopy. Given its putative role in transcriptional regulation, I expected Adn2-GFP to localize to the nucleus. As hypothesized, Adn2p did indeed localize to the nuclear compartment (**Figure 3-11**). To assess Adn2p localization in response to cytokinetic stress, cells were grown as before, but treated with 0.2 μ M LatA for five hours. Adn2p localization was similar to that seen under non-stressed conditions indicating that Adn2p targeting to the nucleus was not affected by LatA treatment (data not shown).

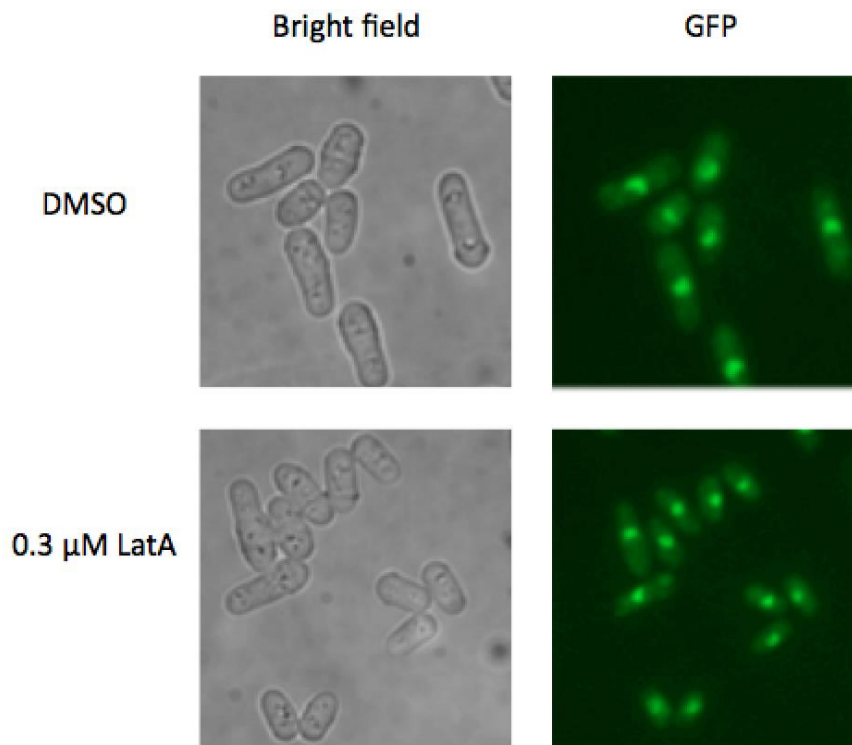


Figure 3-11: Intracellular localization of Adn2p. Adn2p-GFP strains were grown to mid-log phase in liquid EMM-leucine and visualized by bright field (left) and fluorescence microscopy (right) using the GFP filter. Intracellular localization of Adn2p was consistent throughout the cell cycle in both the DMSO treated cells and in cells treated with LatA.

Chapter 4

4 Discussion

4.1 Identifying cytokinesis checkpoint genes

As part of this thesis I performed a genome-wide screen to identify genes involved in the *S. pombe* cytokinesis checkpoint (**Figure 3-1, 3-2**). Version 4 of the Bioneer haploid gene deletion set, which represents ~ 95% of non-essential *S. pombe* genes, was used. The screen was based on the use of the actin depolymerizing drug, Latrunculin A (LatA). LatA is a naturally occurring macrolide toxin produced by the red sea sponge, *Negomabata magnifica* (formerly known as *Latrunculia magnifica*) (Spector et al., 1983). The drug – which consists of a 16-member lactone ring attached to a 2-thiazolidinone moiety – acts within living cells by sequestering G-actin, thereby preventing F-actin assembly (Spector et al., 1983; Coué et al., 1987; Yarmola et al., 2000). *In vitro* studies have shown that LatA binds monomeric actin with a 1:1 stoichiometry and has an equilibrium dissociation constant (K_d) of only ~ 0.2 μM (Coué et al., 1987; Yarmola et al. 2000). When used at high concentrations that are well above its K_d (i.e. 10-50 μM), it is effective in completely disrupting the actin cytoskeleton over a time-frame of minutes (Ayscough, 1998).

While typically used at high concentrations, LatA has also been used at much lower levels (i.e. near the equilibrium constant of 0.2 μM) to mildly perturb the actin cytoskeleton (Coué et al., 1987). In fission yeast, for example, such low dose treatment disrupts the cell division machinery leading to the activation of a cytokinesis checkpoint system (Mishra et al., 2004). This system promotes the establishment of a

cytokinesis competent state characterized by delayed progression into mitosis and the continuous repair and/or re-establishment of the cytokinetic actomyosin ring (reviewed in Karagiannis, 2012). I was thus able to use low dose LatA treatment as an effective tool to perturb the cell division machinery and isolate mutants defective in the cytokinesis checkpoint response. Two mutants previously shown to be hyper-sensitive to LatA (*lsk1* Δ and *pap1* Δ), as well as a wild-type strain, were employed in the screen as positive and negative controls, respectively, to ensure LatA dosage was in the proper range to isolate checkpoint mutants.

4.2 Hypersensitive mutants show varying degrees of sensitivity to LatA

Having identified strains that show a hypersensitive phenotype in response to LatA, I next wanted to further characterize each mutant's sensitivity to the drug. I performed a series of ten-fold serial dilutions to gauge each mutant's sensitivity to LatA. Sensitivity ranged from mild (capable of growth in 0.3 μ M LatA) to severe (incapable of growth in 0.1 μ M LatA) within the group of 38 high confidence hits (**Figure 3-3**). Next, to provide a quantitative assessment of LatA sensitivity, I performed disk diffusion assays where the zone of inhibition for each strain was determined, and used to create a ranked list of the mutants according to their degree of sensitivity to LatA (**Figure 3-4, Table 3-1**). Lastly, the minimum inhibitory concentration (the lowest concentration of LatA that prevented visible colony growth) was determined for each of the 38 strains (**Table 3-2**). The minimum inhibitory concentration varied from 0.2 μ M for wild type to 0.025 μ M for the most sensitive mutants.

Based on this last result I conclude that LatA tolerance is genetically controlled over at least an 8-fold range in *S. pombe*. Importantly, while clear that the identified mutants display growth defects in the presence of the drug, they are nonetheless fully capable of growth and cell division when not stressed (i.e. when grown in the presence of the solvent control, DMSO). These results strongly suggest that fission yeast employ a diverse set of regulatory modules to actively counter cytoskeletal perturbations, thereby ensuring cell survival and proliferation.

It is also clear that these diverse regulatory modules represent a wide-ranging array of biological functions (**Appendix A**). While genes involved in regulating cytokinesis and/or the actin cytoskeleton are indeed represented (e.g. the alpha-actinin gene, *ain1*, the F-actin capping subunit, *acp2*, and the contractile ring protein, *imp2*) (Li et al., 2016; Nakano and Mabuchi, 2006; Ren et al., 2015), other functions, ranging from histone modification to intracellular transport to glucose mediated signaling are also implicated. How these modules interact and communicate to create a cellular state conducive to cytokinesis remains to be determined and will undoubtedly require further experimentation using a broad, multidisciplinary, and systems-based approach. Since such a detailed characterization would be well beyond the scope of a single MSc project, I next decided to focus on a single gene. Due to my interest in transcriptional control, I selected the most highly ranked transcription factor from the high-confidence list of hits, *adn2* (for adhesion defective).

4.3 Adn2p is required for ring constriction upon LatA treatment

My initial assays demonstrated that the *adn2Δ* mutant was defective in cytokinesis, however the assays did not show why cell division failed. Since one of the responses of the cytokinetic monitoring system is to stabilize the actomyosin ring, I observed actomyosin ring dynamics in *adn2Δ* mutants (**Figure 3-9**). To observe ring constriction I used strains expressing the Rlc1p-GFP fusion protein. Rlc1p is a myosin regulatory light chain that binds two Type II myosin heavy chains, which are responsible for ring formation. Therefore Rlc1p-GFP fusion proteins can be used to monitor actomyosin ring constriction in live cells and in real time.

Upon treatment with DMSO, both *adn2Δ* cells and wild-type cells displayed similar ring constriction kinetics, taking on average 30-35 minutes to assemble and constrict the actomyosin ring. Upon treatment with 0.2 μM LatA, wild-type cells were still able to assemble and constrict the ring, however this occurred over a longer period of time, taking about 70 minutes to complete. When treated with LatA, the mutant *adn2Δ* displayed different ring dynamics. While able to initially assemble the ring, ring expression became progressively weaker, and eventually faded from view over a time-frame of 30-35 minutes. These results suggest that Adn2p is not an essential component of ring assembly, but is required for proper constriction when the cell division machinery is perturbed. This phenotype is somewhat in contrast to other LatA sensitive mutants (e.g. *lsk1Δ*, *clp1Δ*) where the ring visibly fragments into multiple pieces upon LatA treatment (Karagiannis et al., 2005; Mishra et al., 2004). How Adn2p (or other LatA sensitive mutants) affect actomyosin ring structure and constriction remains unknown and will be the subject of future research. Considering Adn2p's role

as a transcription factor, it would be interesting to use gene expression profiling (+/- LatA) to determine whether *adn2Δ* mutants display defects in the expression of genes involved in actin ring assembly or constriction.

4.4 The Adn2p transcription factor localizes to the nucleus

Since *adn2* is a predicted transcription factor, I hypothesized that Adn2p would localize to the nucleus. To assess localization, I transformed a plasmid containing the carboxy terminus of *adn2* fused upstream of the GFP coding sequence. This construct was then homologously integrated at the *adn2* locus so that expression was controlled by the native promoter. As expected, Adn2p was observed to localize to the nucleus (**Figure 3-11**).

Interestingly, a previous high throughput study reported that Adn2p localized to cytoplasmic dots (Matsuyama et al., 2006). However, in the study by Matsuyama et al. Adn2p was expressed under the control of the strong *nmt1* promoter. It is thus possible that the cytoplasmic dots observed in that study are simply the result of the abnormally high level of expression leading to the formation of artefactual protein aggregates. It should be noted that in my study *adn2* was expressed under the control of its native promoter, and thus my results more likely reflect the true localization of the protein *in vivo*. The fact that Adn2p is a transcription factor, and must enter the nucleus to function, also supports the results of my localization studies.

4.5 Overexpression of Adn2p results in cytokinetic abnormalities

To explore the effects of modulating Adn2p dosage on cytokinesis, I overexpressed the protein using the pREP series of expression vectors (**Figure 3-10**). Interestingly, cells overexpressing Adn2p via the *nmt1* promoter accumulated abnormal cells with multiple septa, while cells under the control of the weaker *nmt41* and *nmt81* promoters did not accumulate cells with multiple septa. This result implies that overexpression of *adn2* results in a dominant-negative effect in which the abnormally high levels of Adn2p adversely affects the normal functioning of Adn2p and/or its associated protein partners within the cell and thus giving rise to the abnormal multi-septate phenotype. A dominant-negative effect is also supported by the fact that, similar to *adn2Δ* mutants, cells overexpressing Adn2p are hyper-sensitive to LatA (data not shown). A dominant negative effect is the result of a protein masking the effect of the wild type endogenous protein, resulting in loss of wild-type protein function and phenotype. Given the role of Adn2p as a transcription factor, it is possible that the high levels of Adn2p results in the ectopic expression of target genes involved in cytokinesis thereby resulting in the improper stoichiometry of the protein complexes governing cell division. Gene expression profiling (+/- LatA) would be one method by which to definitively test this hypothesis.

4.6 Adn2p might be part of a multi-protein complex with roles in defending against cytoskeletal perturbations

The BioGrid database (www.thebiogrid.org/) was queried to identify Adn2p binding partners. This analysis revealed a small interactome of three proteins: the

importin- α , Imp1p, autophagy associated protein, Atg24p, and the uncharacterized protein, SPBC354.04 (**Figure 3-8**). Interestingly, two of the genes, *imp1* and *atg24* were identified as hits in this study. A detailed analysis of the functional role of each of the three proteins suggests the multi-protein complex might have a role in defending against cytoskeletal perturbations.

Imp1p is an importin- α that is involved in the import of proteins targeted to the nucleus. In *S. pombe*, Imp1p localizes to nuclear pores at the nuclear envelope throughout the cell cycle and during cell division when the nuclear envelope surrounds the elongating mitotic spindle (Lucena et al., 2015). Imp1p acts as an adaptor protein, interacting with cargo proteins in the cytoplasm, linking the cargo protein to an importin- β , and then migrating into the nucleoplasm through a nuclear pore (Lucena et al., 2015). *S. pombe* Imp1p has been shown to interact with the AP-1-like transcription factor Pap1p, which is involved in multidrug resistance by regulating genes required in multiple stress response pathways (Umeda et al., 2005). The *pap1 Δ* strain is used in this study as a positive control as it is a mutant known to be hypersensitive to a wide variety of toxins and which was observed to be highly sensitive to LatA (Asadi et al., 2017). As expected, due to its interaction with Imp1p, Pap1p contains an NLS sequence (Umeda et al., 2005). Furthermore, Pap1p translocates into the nucleus in an Imp1p dependent manner (Asadi et al., 2017). Interestingly, the Adn2p protein sequence also contains an NLS sequence: KRHKR (Kosugi et al., 2008). It would thus be interesting to determine whether Adn2p localization to the nucleus is also dependent on Imp1p.

Also included in the multi-protein complex is Atg24p. Atg24p belongs to the Autophagy related (Atg) protein family, members of which are involved in autophagy. Autophagy has been extensively studied in *S. cerevisiae*, and many homologs of the autophagy machinery required in *S. cerevisiae* have been identified in *S. pombe*. The predicted function of *atg24* in *S. pombe* has largely been inferred from sequence homology with *S. cerevisiae* Atg24p (Mukaiyama, et al., 2010; Zhao et al., 2016). Atg24p binds to the membrane phospholipids phosphatidylinositol-3-phosphate via its PX domain and localizes to membrane structures involved in autophagy. Recently, a study in *S. pombe* found that Atg24p localizes to a pre-autophagosomal structure called the phagophore assembly site (PAS). The study also found that Atg24p is required for selective autophagy in *S. pombe*, which targets specific cargos for degradation via receptor recognition. Specifically, Atg24p is involved in the cytoplasm to vacuole targeting (Cvt) pathway, which delivers the hydrolase α - aminopeptidase I (Ape1) to the vacuole (Zhao et al., 2016). This pathway is exclusively found in yeast, and the exact function of Atg24p in the Cvt pathway in both budding and fission yeast remains unknown.

The last Adn2p binding partner is the *S. pombe* specific protein, SPBC354.04. SPBC354.04 is a short, 163 amino acid long protein that is thought to localize to the cytosol and nucleus (Matsuyama et al., 2006). Interestingly, SPBC354.04 has been predicted to interact with the autophagy-related protein Atg11 (Vo et al., 2016). In *S. pombe* *atg11* is part of the core Cvt machinery, directing receptor bound cargo to the PAS (Yamasaki A et al., 2017). Interestingly, the process of autophagy has indeed been linked to successful cytokinesis (Belaid et al., 2013). In this study, the authors

show that inhibition of autophagosome formation result in cytokinesis failure, multinucleation, and aneuploidy in mouse renal cells. The possible role of Adn2p in regulating autophagy, and the role of autophagy in fission yeast cytokinesis, remains unknown and will require further study.

4.7 Adn2p target genes include cell wall remodeling enzymes

Adhesion defective protein 2 (Adn2p) was first identified in *S. pombe* during a screen for haploid deletion strains unable to invade the growth medium. Invasion of medium by yeast cells required flocculant growth, a type of cellular growth exhibited by yeast in which they form elaborate, branched, multicellular structures which deeply invade the growth medium. Prior to the visible invasion of the medium, cells adhere to the surface of the medium and become resistant to removal by gentle washing. *Adn2Δ* strains were defective in this first step of invasive growth, and did not adhere to the medium, and based on this phenotype the gene was named adhesion defective protein (Dodson et al., 2009).

Sequence analysis found that *adn2* is orthologous to *S. cerevisiae* FLO8 (**Figure 3-7**), a transcription factor required for flocculation and invasive growth. Similar to FLO8, Adn2p contains a LisH domain, suspected to be required for protein dimerization (Mateja et al., 2006; Kim et al., 2014). Also found within Adn2p are a ssDNA binding domain, and two coiled coil domains (**Figure 3-6**), both of which further implicate Adn2p as a regulator of transcription.

Since its identification in the flocculation screen performed by Dodgson and colleagues in 2009, no further characterization of Adn2p was reported in the literature, until a more recent study by Kwon and colleagues (2012). In their effort to uncover the

transcriptional-regulatory network of flocculation in *S. pombe*. the group uncovered Adn2p as one of the master regulators of flocculation in the fission yeast.

Kwon et al. (2012) observed that *adn2* overexpression was sufficient to trigger flocculation (FLO8 overexpression in budding yeast also triggers flocculation). However, unlike its budding yeast ortholog, which targets the flocculin genes (FLO1 and FLO11), the flocculent phenotype of Adn2p overexpression is attributed to the expression of cell-wall remodeling enzymes (Teunissen and Steensma, 1995; Kwon et al., 2012). Microarray analysis uncovered that Adn2p overexpression triggers up-regulation of two cell-wall remodeling enzymes, *gas2*⁺ (a glycosyltransferase) and SPAC4H3.03c (a glycoside hydrolase). Cell wall remodeling is an essential process for proper growth and adaptation to environmental stresses in yeast cells. Part of the cell wall remodeling process involves dissolution of sugar moieties in the glucan layer by glycoside hydrolases and elongation of glucan chains by glycosyltransferases. The role of *gas2*⁺ and SPAC4H3.03c in flocculation may be to restructure the cell wall, which may result in the rearrangement of flocculins, making them more accessible to cell surface oligosaccharides (Kwon et al., 2012).

Similar to the multiseptate overexpression phenotype of Adn2p observed in my study, Kwon et al. (2012) observed the same multisepta phenotype when Adn2p was overexpressed. The multisepta phenotype was not observed when *gas2*⁺ and SPAC4H3.03c were overexpressed, suggesting that *adn2* may regulate cell separation and flocculation independently through different sets of target gene. The group further hypothesizes that Adn2p may control septation via *ace2*⁺, a transcriptional activator of the cell division process, and identified in my study as a low confidence hit (Appendix

1). Therefore, targets of the Adn2p transcription factor include genes controlling septation as well as cell wall remodeling genes (Kwon et al., 2012). Further work will need to be done to determine the critical transcriptional targets of Adn2p with respect to the phenotypes described in this study.

4.8 Future work concerning the role of Adn2p in defending against cytoskeletal perturbations

In this study, we have shown that Adn2p is necessary for cell survival when cells are exposed to cytokinetic stress. However, we do not know the mechanism through which Adn2p ensures the faithful execution of cytokinesis in the presence of LatA. Identifying the genes that Adn2p regulates in order to ensure the accurate and reliable execution of cytokinesis would provide insight into the role of Adn2p in the cytokinesis checkpoint. This could be accomplished through gene expression profiling of both wild-type and *adn2Δ* mutant fission yeast in the presence and absence of LatA.

We have shown that Adn2p has a role in defending against cytokinetic stress during cell division, however, does Adn2p have a role in defending against other cytoskeletal perturbations? Based on the individual gene functions of the predicted Adn2p interactome, Adn2p may be involved in defending against cytoskeletal perturbation in the Cvt pathway. Further experiments are needed to confirm the Adn2p interactome. A co-immunoprecipitation assay could confirm if the predicted interactome exists *in vivo*, however if the interactome is only required for the Cvt pathway, it may be difficult to isolate, as little is known about the cellular conditions required to induce the Cvt pathway *in vitro*.

We have shown that Adn2p is required for the execution of cytokinesis in the presence of LatA. Adn2p has also been implicated in surface adhesion during

flocculation (Dodgson et al., 2009) and as a transcriptional activator of cell wall remodeling enzymes (Kwon et al., 2012). With this emerging set of diverse cellular functions, Adn2p is a protein that warrants further investigation and will contribute to our overall understanding of multiple cellular processes in *S. pombe*.

Literature Cited

- Almonacid, M., & Paoletti, A.** (2010). Mechanisms controlling division-plane positioning. *Seminars in Cell & Developmental Biology*, *21*(9), 874-880.
- Ayscough, K. R., Stryker, J., Pokala, N., Sanders, M., Crews, P., & Drubin, D. G.** (1997). High rates of actin filament turnover in budding yeast and roles for actin in establishment and maintenance of cell polarity revealed using the actin inhibitor latrunculin-A. *The Journal of Cell Biology*, *137*(2), 399-416.
- Baba, M., Osumi, M., Scott, S.V., Klionsky, D.J., & Ohsumi, Y.** (1997). Two distinct pathways for targeting proteins from the cytoplasm to the vacuole/lysosome, *J. Cell Biol.* *139*, 1687–1695.
- Bähler, J., & Pringle, J. R.** (1998). Pom1p, a fission yeast protein kinase that provides positional information for both polarized growth and cytokinesis. *Genes & Development*, *12*(9), 1356-1370.
- Balasubramanian, M. K., Bi, E., & Glotzer, M.** (2004). Comparative analysis of cytokinesis in budding yeast, fission yeast and animal cells. *Current Biology*, *14*(18), R806-R818.
- Barr, F. A., & Gruneberg, U.** (2007). Cytokinesis: placing and making the final cut. *Cell*, *131*(5), 847-860.
- Basi, G., Schmid, E., & Maundrell, K.** (1993). TATA box mutations in the *Schizosaccharomyces pombe nmt1* promoter affect transcription efficiency but not the transcription start point or thiamine repressibility. *Gene*, *123*, 11–136.
- Bathe, M., & Chang, F.** (2010). Cytokinesis and the contractile ring in fission yeast: towards a systems-level understanding. *Trends in Microbiology*, *18*(1), 38-45.
- Bezanilla, M., Forsburg, S. L., & Pollard, T. D.** (1997). Identification of a second myosin-II in *Schizosaccharomyces pombe*: Myp2p is conditionally required for cytokinesis. *Molecular Biology of the Cell*, *8*(12), 2693-2705.
- Celton-Morizur, S., Racine, V., Sibarita, J. B., & Paoletti, A.** (2006). Pom1 kinase links division plane position to cell polarity by regulating Mid1p cortical distribution. *Journal of Cell Science*, *119*(22), 4710-4718.
- Coué M., Brenner S. L., Spector I., Korn E. D.** (1987). Inhibition of actin polymerization by latrunculin A. *FEBS Lett.*, *213*(2), 316–318.
- Daga, R. R., & Chang, F.** (2005). Dynamic positioning of the fission yeast cell division plane. *Proceedings of the National Academy of Sciences of the United States of America*, *102*(23), 8228-8232.

- Daniels, M. J., Wang, Y., Lee, M., & Venkitaraman, A. R.** (2004). Abnormal cytokinesis in cells deficient in the breast cancer susceptibility protein BRCA2. *Science*, 306(5697), 876-879.
- Dodgson, J., Avula, H., Hoe, K-L., Kim, D-U., Park, H-O., Hayles, J., and Armstrong, J.** (2009). Functional Genomics of Adhesion, Invasion, and Mycelial Formation in *Schizosaccharomyces pombe*. *Eukaryot. Cell*. 8(8), 1298 – 1306.
- Eggert, U. S., Mitchison, T. J., & Field, C. M.** (2006). Animal cytokinesis: from parts list to mechanisms. *Annual Review of Biochemistry*, 75, 543-66.
- Lucena, R., Dephoure, N., Gygi, S.P., Kellogg, D.R., Tallada, V.A., Daga, R.R., and Jimenez, J.** (2015). Nucleocytoplasmic transport in the midzone membrane domain controls yeast mitotic spindle disassembly. *J. Cell Biol.* 209(3) 387 – 402.
- Lynch-Day, M.A., and Klionsky, D.J.** (2010). The Cvt pathway as a model for selective autophagy. *FEBS Lett.* 584(7): 1359–1366.
- Fededa, J. P., and Gerlich D.W.** (2012). Molecular control of animal cell cytokinesis. *Nature Cell Biology*. (14) 440–447.
- Forsburg, S. L., & Rhind, N.** (2006). Basic methods for fission yeast. *Yeast*, 23(3), 173- 183.
- Fujiwara, T., Bandi, M., Nitta, M., Ivanova, E. V., Bronson, R. T., & Pellman, D.** (2005). Cytokinesis failure generating tetraploids promotes tumorigenesis in p53⁻ null cells. *Nature*, 437(7061), 1043-1047.
- Ganem, N. J., Storchova, Z., & Pellman, D.** (2007). Tetraploidy, aneuploidy and cancer. *Current Opinion in Genetics & Development*, 17(2), 157-162.
- Gerlitz, G., Darhin, E., Giorgio, G., Franco, B., and Reiner, O.** (2005) Novel Functional Features of the LIS-H Domain: Role in Protein Dimerization, Half-Life and Cellular Localization, *Cell Cycle*, 4(11), 1632-1640.
- Glotzer, M.** (2001). Animal cell cytokinesis. *Annual Review of Cell and Developmental Biology*, 17(1), 351-386.
- Glotzer, M.** (2005). The molecular requirements for cytokinesis. *Science*, 307(5716), 1735-1739.
- Gould, K.L., & Simanis, V.** (1997). The control of septum formation in fission yeast. *Genes & Development*. 11:2939–2951.
- Guertin, D. A., Trautmann, S., & McCollum, D.** (2002). Cytokinesis in eukaryotes. *Microbiology and Molecular Biology Reviews*, 66(2), 155-178.
- Harris, H.** (2008). Concerning the origin of malignant tumours by Theodor Boveri. Translated and annotated by Henry Harris. *Journal of cell science*, 121(Supplement 1), 1-84

- Hartwell, L. H., & Weinert, T. A.** (1989). Checkpoints: controls that ensure the order of cell cycle events. *Science*, 246(4930), 629-634.
- Holland, A. J., & Cleveland, D. W.** (2009). Boveri revisited: chromosomal instability, aneuploidy and tumorigenesis. *Nature Reviews Molecular Cell Biology*, 10(7), 478-487.
- Hou, M. C., Salek, J., & McCollum, D.** (2000). Mob1p interacts with the Sid2p kinase and is required for cytokinesis in fission yeast. *Current Biology*, 10(10), 619-622.
- Huang, Y., T.G. Chew, W. Ge, & Balasubramanian, M.K.** (2007). Polarity determinants Tea1p, Tea4p, and Pom1p inhibit division-septum assembly at cell ends in fission yeast. *Developmental Cell*, 12(6) 987–996.
- Karagiannis, J., Bimbó, A., Rajagopalan, S., Liu, J., & Balasubramanian, M. K.** (2005). The nuclear kinase Lsk1p positively regulates the septation initiation network and promotes the successful completion of cytokinesis in response to perturbation of the actomyosin ring in *Schizosaccharomyces pombe*. *Molecular Biology of the Cell*, 16(1), 358-371.
- Karagiannis, J., & Balasubramanian, M. K.** (2007). A cyclin-dependent kinase that promotes cytokinesis through modulating phosphorylation of the carboxy terminal domain of the RNA Pol II Rpb1p sub-unit. *PLoS ONE*, 2(5), e433.
- Karagiannis, J.** (2012). Ensuring the faithful execution of cytokinesis in *Schizosaccharomyces pombe*. *Communicative & Integrative Biology*, 5(3), 265- 271.
- Kim, D. U., Hayles, J., Kim, D., Wood, V., Park, H. O., Won, M., ... & Hoe, K. L.** (2010). Analysis of a genome-wide set of gene deletions in the fission yeast *Schizosaccharomyces pombe*. *Nature Biotechnology*, 28(6), 617-623.
- Kim, H.Y., Lee, S.B., Kang, H.S., Oh, G.T., and Kim, T.** (2014). Two distinct domains of Flo8 activator mediates its role_{SEP} in transcriptional activation and the physical interaction with Mss11. 449, 202 – 207.
- Kitayama, C., Sugimoto, A., & Yamamoto, M.** (1997). Type II myosin heavy chain encoded by the *myo2* gene composes the contractile ring during cytokinesis in *Schizosaccharomyces pombe*. *The Journal of Cell Biology*, 137(6), 1309-1319.
- Kosugi, S., Hasebe, M., Tomita, M., Yanagawa, H.** (2008). Nuclear export signal consensus sequences defined using a localization-based yeast selection system. *Traffic*, 9, 2053–2062.
- Kovar, D. R., Kuhn, J. R., Tichy, A. L., & Pollard, T. D.** (2003). The fission yeast cytokinesis formin Cdc12p is a barbed end actin filament capping protein gated by profilin. *The Journal of Cell Biology*, 161(5), 875-887.
- Krapp, A., & Simanis, V.** (2008). An overview of the fission yeast septation initiation network (SIN). *Biochemical Society Transactions*, 36(3), 411-415.

- Kwon, E-J. G., Laderoute, A., Chatfield-Reed, Lianne Vachon, L., Karagiannis, J., and Chua, G.** (2012). *PLoS Genet* 8(12), e1003104.
- Le Goff, X., Motegi, F., Salimova, E., Mabuchi, I., & Simanis, V.** (2000). The *S. pombe* *rlc1* gene encodes a putative myosin regulatory light chain that binds the type II myosins myo3p and myo2p. *Journal of Cell Science*, 113(23), 4157-4163.
- Le Goff, X., Woollard, A., & Simanis, V.** (1999). Analysis of the *cps1* gene provides evidence for a septation checkpoint in *Schizosaccharomyces pombe*. *Molecular and General Genetics*, 262(1), 163-172.
- Lee, M. G., and Nurse, P.**(1987). Complementation used to clone a human homolog of the fission yeast cell cycle control gene *cdc2⁺*. *Nature*, 327, 31-35.
- Li Y., Christensen J. R., Homa K. E., Hocky G. M., Fok A., et al.** (2016). The F-actin bundler α -actinin Ain1 is tailored for ring assembly and constriction during cytokinesis in fission yeast. *Mol. Biol. Cell*, 27(11), 1821–1833.
- Liu, J., Wang, H., & Balasubramanian, M. K.** (2000). A checkpoint that monitors cytokinesis in *Schizosaccharomyces pombe*. *Journal of Cell Science*, 113(7), 1223-1230.
- Lv, L., Zhang, T., Yo, Q., Huang, Y., Wang, Z., Hou, H., Zhang, H., Zhang, W., Guo, Z., Cooke, H.J., and Shi, Q. et al.** (2012). Tetraploid cells from cytokinesis failure induce aneuploidy and spontaneous transformation of mouse ovarian surface epithelial cells. *Cell Cycle*, 11(15), 2864-2875.
- Mateja, A., Cierpicki, T., Paduch, M., Derewenda, Z.S., and Otlewski, J.** (2006). The dimerization mechanism of LIS1 and its implication for proteins containing the LisH motif. *J. Mol. Biol.* 357(2): 621–31.
- Matsuyama, A., Shirai, A., Yashiroda, Y., Kamata, A., Horinouchi, S., Yoshida, M.** (2004). pDual, multipurpose, multicopy vector capable of chromosomal integration in fission yeast. *Yeast*. 21(15), 1289-1305.
- Matsuyama, A., Arai, R., Yashiroda, Y., Shirai, A., Kamata, A., Sekido, S., ... & Yoshida, M.** (2006). ORFeome cloning and global analysis of protein localization in the fission yeast *Schizosaccharomyces pombe*. *Nature Biotechnology*, 24(7), 841-847.
- Maudrell, K.** (1990). *nmt1* of fission yeast. A highly transcribed gene completely repressed by thiamine. *Journal of Biological Chemistry*, 265(19), 10857-10864.
- May, K. M., Watts, F. Z., Jones, N., & Hyams, J. S.** (1997). Type II myosin involved in cytokinesis in the fission yeast, *Schizosaccharomyces pombe*. *Cell Motility and the Cytoskeleton*, 38(4), 385-396
- Mishra, M., Karagiannis, J., Trautmann, S., Wang, H., McCollum, D., & Balasubramanian, M. K.** (2004). The Clp1p/Flp1p phosphatase ensures completion of

- cytokinesis in response to minor perturbation of the cell division machinery in *Schizosaccharomyces pombe*. *Journal of Cell Science*, 117(17), 3897-3910.
- Mishra, M., Karagiannis, J., Sevugan, M., Singh, P., & Balasubramanian, M. K.** (2005). The 14-3-3 protein rad24p modulates function of the cdc14p family phosphatase clp1p/flp1p in fission yeast. *Current Biology*, 15(15), 1376-1383.
- Morgan, D. O.** (1997). Cyclin-dependent kinases: engines, clocks, and microprocessors. *Annual Review of Cell and Developmental Biology*, 13(1), 261-291.
- Moseley, J. B., Mayeux, A., Paoletti, A., & Nurse, P.** (2009). A spatial gradient coordinates cell size and mitotic entry in fission yeast. *Nature*, 459(7248), 857- 860.
- Mukaiyama, H., Nakase, M., Nakamura, T., , Kakinuma, Y., Takegawa. K.** (2010). Autophagy in the fission yeast *Schizosaccharomyces pombe*. *FEBS Lett.* 584, 1327 – 1442.
- Nakano K., Mabuchi I.** (2006). Actin-capping protein is involved in controlling organization of actin cytoskeleton together with ADF/cofilin, profilin and F-actin crosslinking proteins in fission yeast. *Genes Cells*, 11(8), 893–905.
- Nurse, P., Thuriaux, P., & Nasmyth, K.** (1976). Genetic control of the cell division cycle in the fission yeast *Schizosaccharomyces pombe*. *Molecular and General Genetics MGG*, 146(2), 167-178.
- Nurse, P., & Thuriaux, P.** (1980). Regulatory genes controlling mitosis in the fission yeast *Schizosaccharomyces pombe*. *Genetics*, 96(3), 627-637.
- Olaharski, A. J., Sotelo, R., Solorza-Luna, G., Gonsebatt, M. E., Guzman, P., Mohar, A., & Eastmond, D. A.** (2006). Tetraploidy and chromosomal instability are early events during cervical carcinogenesis. *Carcinogenesis*, 27(2), 337-343.
- Prekeris, R., & Gould, G. W.** (2008). Breaking up is hard to do—membrane traffic in cytokinesis. *Journal of Cell Science*, 121(10), 1569-1576.
- Pollard, T. D., & Wu, J. Q.** (2010). Understanding cytokinesis: lessons from fission yeast. *Nature Reviews Molecular Cell Biology*, 11(2), 149-155.
- Rappaport, R.** (1996). Cytokinesis in animal cells. In *Developmental and cell biology series* 32. Cambridge University Press, New York, NY. 386.
- Reggiori, R., Monastyrska, I., Shintani, T., and Klionsky, D.** (2005). The Actin Cytoskeleton Is Required for Selective Types of Autophagy, but Not Nonspecific Autophagy, in the Yeast *Saccharomyces cerevisiae*. *Molecular Cell Biology*, 16: 5843–5856.
- Ren L., Willet A. H., Roberts-Galbraith R. H., McDonald N. A., Feoktistova A., et al.,** (2015). The Cdc15 and Imp2 SH3 domains cooperatively scaffold a network of proteins

that redundantly ensure efficient cell division in fission yeast. *Mol. Biol. Cell*, 26(2), 256–269.

Schmidt S., Sohrmann M., Hofmann K., Woollard A., Simanis V. (1997) The Spg1p GTPase is an essential, dosage-dependent inducer of septum formation in *Schizosaccharomyces pombe*. *Genes & Development*, 11, 1519–1534.

Simanis V. (1995) The control of septum formation and cytokinesis in fission yeast. *Seminars in Cell Biology*, 6(2), 79–87

Skop, A. R., Liu, H., Yates, J., Meyer, B. J., & Heald, R. (2004). Dissection of the mammalian midbody proteome reveals conserved cytokinesis mechanisms. *Science*, 305(5680), 61-66.

Spector I., Shochet N. R., Kashman Y., Groweiss A. (1983). Latrunculins: novel marine toxins that disrupt microfilament organization in cultured cells. *Science*, 219(4584), 493–495.

Teunissen A.U.R.H., and Stwensma, H.Y. (1995). Review: The Dominant Flocculation Genes of *Saccharomyces cerevisiae* Constitute a New Subtelomeric Gene Family. *Yeast*, 11, 1001 – 1013.

Tomlin, G. C., Morrell, J. L., & Gould, K. L. (2002). The spindle pole body protein Cdc11p links Sid4p to the fission yeast septation initiation network. *Molecular Biology of the Cell*, 13(4), 1203-1214.

Trautmann, S., Wolfe, B. A., Jorgensen, P., Tyers, M., Gould, K. L., & McCollum, D. (2001). Fission yeast Clp1p phosphatase regulates G2/M transition and coordination of cytokinesis with cell cycle progression. *Current Biology*, 11(12), 931-940.

Umeda, M., Izaddoost, S., Cushman, I., Moore, M.S., and Sazer, S. (2005). The Fission Yeast *Schizosaccharomyces pombe* Has Two Importin-a Proteins, Imp1p and Cut15p, Which Have Common and Unique Functions in Nucleocytoplasmic Transport and Cell Cycle Progression. *Genetics*, 171, 7 – 12.

Vo, T.V., Das, J., Meyer, M.J., Cordero, N.A., Akturk, N., Wei, X., Fairm B.J., Degatano, A.G., Fragoza, R., Liu, L.G., Matsuyama, A., Trickey, M., Horibata, S, Grimson, A., Yamano, H., Yoshida, M., Roth, F.P., Pleiss, J.A., Xia, Y., and Yu, H.(2016). A proteome-wide fission yeast interactome reveals network evolution principles from yeasts to humans. *Cell*, 164(1-2):310 – 323.

Wood, V., Gwilliam, R., Rajandream, M. A., Lyne, M., Lyne, R., Stewart, A., ... & Pearson, D. (2002). The genome sequence of *Schizosaccharomyces pombe*. *Nature*, 415(6874), 871-880.

Wolfe, B. A., & Gould, K. L. (2005). Split decisions: coordinating cytokinesis in yeast. *Trends in Cell Biology*, 15(1), 10-18.

- Wu, J. Q., & Pollard, T. D.** (2005). Counting cytokinesis proteins globally and locally in fission yeast. *Science*, *310*(5746), 310-314.
- Wu, J. Q., Sirotkin, V., Kovar, D. R., Lord, M., Beltzner, C. C., Kuhn, J. R., & Pollard, T. D.** (2006). Assembly of the cytokinetic contractile ring from a broad band of nodes in fission yeast. *The Journal of Cell Biology*, *174*(3), 391-402.
- Yamasaki, A., and Noda, N.N.** (2017). Structural Biology of the Cvt pathway. *J. Mol. Biol.*, *429*(4), 531 – 542.
- Yanagida, M.** (2002). The model unicellular eukaryote, *Schizosaccharomyces pombe*. *Genome Biology*, *3*(3), 2003.1–2003.4.
- Yarmola E. G., Somasundaram T., Boring T. A., Spector I., Bubb M. R.** (2000). Actin-latrunculin A structure and function: differential modulation of actin-binding protein function by latrunculin A. *J. Biol. Chem.*, *275*, 28120–28127.
- Yoshida, M., & Sazer, S.** (2004). Nucleocytoplasmic transport and nuclear envelope integrity in the fission yeast *Schizosaccharomyces pombe*. *Methods*, *33*(3), 226- 238.
- Zhao, D., Liu, X., Yu, Z-Q., Sun, L-L, Xiong, X., Dong, M-Q., and Du, L-L.** (2016). Atg20- and Atg24-family proteins promote organelle autophagy in fission yeast. *J. Cell Sci.* *129*, 4289 – 4304.

Appendices

Appendix A: Complete list of LatA sensitive gene deletion mutants identified via genome-wide screening. “Y” indicates that the gene was hit in a given trial of the screen. “n” indicates that the gene was not hit in a given trial of the screen.

Systemic ID	Gene description	Trial #1	Trial #2	Trial #3	Confidence
SPAC15A10.08	alpha-actinin	Y	Y	Y	High
SPAC167.01	Ppk4 sensor	Y	Y	Y	High
SPAC17A5.14	exonuclease II Exo2	Y	Y	Y	High
SPAC19A8.04	C-22 sterol desaturase Erg5	Y	Y	Y	High
SPAC3H8.08c	transcription factor (predicted)	Y	Y	Y	High
SPAC4G9.14	Mvp17/PMP22 family protein 2	Y	Y	Y	High
SPAC57A7.04c	mRNA export shuttling protein	Y	Y	Y	High
SPAC630.14c	transcriptional corepressor Tup12	Y	Y	Y	High
SPAC631.01c	F-actin capping protein beta subunit	Y	Y	Y	High
SPAC688.11	Huntingtin-interacting protein homolog	Y	Y	Y	High
SPAC6F6.01	calcium channel Cch1	Y	Y	Y	High
SPAC869.11	cationic amino acid transporter Cat1	Y	Y	Y	High
SPAC9.02c	polyamine N-acetyltransferase	Y	Y	Y	High
SPBC106.10	Pka1	Y	Y	Y	High
SPBC11C11.02	contractile ring protein Imp2	Y	Y	Y	High
SPBC1289.10c	transcription factor (predicted)	Y	Y	Y	High
SPBC19C7.01	Mago binding protein homolog	Y	Y	Y	High
SPBC215.04	Git11	Y	Y	Y	High
SPBC28F2.10c	SAGA complex subunit Ngg1	Y	Y	Y	High
SPBC3D6.02	But2 family protein But2	Y	Y	Y	High
SPBC4F6.06	Kin1	Y	Y	Y	High
SPBP16F5.03c	Tra1	Y	Y	Y	High
SPCC1020.07	haloacid dehalogenase-like hydrolase	Y	Y	Y	High
SPCC1753.02c	G-protein coupled receptor Git3	Y	Y	Y	High
SPCC4F11.03c	sequence orphan	Y	Y	Y	High
SPCC645.08c	RNA-binding protein Snd1	Y	Y	Y	High
SPCC70.06	nuclear export factor	Y	Y	Y	High
SPCC794.08	HEAT repeat protein	Y	Y	Y	High
SPAC16C9.06c	ATP-dependent RNA helicase Upf1	Y	Y	Y	High
SPAC3C7.07c	arginine-tRNA protein transferase	Y	Y	Y	High
SPBC13G1.03c	peroxisomal docking protein Pex14	Y	Y	Y	High
SPBC32H8.07	Git5	Y	Y	Y	High
SPBC651.11c	AP-3 adaptor complex subunit Apm3	Y	Y	Y	High
SPBC725.10	tspO homolog	Y	Y	Y	High

SPCC162.10	serine/threonine protein kinase Ppk33	Y	Y	Y	High
SPCC285.09c	cAMP-specific phosphodiesterase Cgs2	Y	Y	Y	High
SPCC297.05	diacylglycerol binding protein	Y	Y	Y	High
SPCC794.03	amino acid permease (predicted)	Y	Y	Y	High
SPAC12B10.07	F-actin capping protein alpha subunit	Y	n	Y	Medium
SPAC13C5.04	amidotransferase (predicted)	n	Y	Y	Medium
SPAC144.06	AP-3 adaptor complex subunit Apl5	Y	n	Y	Medium
SPAC1952.05	Gcn5	Y	n	Y	Medium
SPAC19B12.10	human AMSH/STAMBIP protein homolog	n	Y	Y	Medium
SPAC19E9.02	NIMA related Fin1	Y	n	Y	Medium
SPAC1D4.03c	autophagy associated protein Aut12	Y	n	Y	Medium
SPAC227.10	prefoldin subunit 2	Y	n	Y	Medium
SPAC22A12.04c	40S ribosomal protein S15a	Y	n	Y	Medium
SPAC22E12.11c	Set3	Y	n	Y	Medium
SPAC23A1.11	60S ribosomal protein L13/L16	n	Y	Y	Medium
SPAC23H3.13c	Gpa2	Y	n	Y	Medium
SPAC24B11.12c	P-type ATPase	Y	n	Y	Medium
SPAC26A3.04	60S ribosomal protein L20	Y	Y	n	Medium
SPAC26A3.06	rRNA (guanine) methyltransferase	Y	n	Y	Medium
SPAC26A3.16	UBA domain protein Dph1	Y	n	Y	Medium
SPAC26F1.04c	enoyl-[acyl-carrier protein] reductase	Y	n	Y	Medium
SPAC27E2.03c	GTP binding protein	n	Y	Y	Medium
SPAC29A4.20	Elp3	Y	n	Y	Medium
SPAC29B12.08	sequence orphan	Y	n	Y	Medium
SPAC30.02c	Kti2	Y	n	Y	Medium
SPAC30D11.05	Aps3	Y	n	Y	Medium
SPAC31A2.16	RhoGEF Gef2	Y	n	Y	Medium
SPAC31G5.19	ATPase with bromodomain protein	Y	n	Y	Medium
SPAC323.04	mitochondrial ATPase	n	Y	Y	Medium
SPAC328.10c	40S ribosomal protein S5	Y	n	Y	Medium
SPAC4C5.02c	GTPase Ryh1	Y	n	Y	Medium
SPAC6F6.12	autophagy associated protein Atg24	Y	n	Y	Medium
SPAC8E11.02c	14-3-3 protein Rad24	Y	n	Y	Medium
SPAC959.08	60S ribosomal protein L21	Y	n	Y	Medium
SPAPB17E12.03	ubiquitin-protein ligase E3	Y	n	Y	Medium
SPAPB1E7.02c	Mcl1	n	Y	Y	Medium
SPBC1105.04c	CENP-B homolog	Y	n	Y	Medium
SPBC119.08	MAP kinase Pmk1	Y	n	Y	Medium
SPBC11B10.07c	CDC50 domain protein	Y	n	Y	Medium
SPBC11C11.08	SR family protein Srp1	Y	n	Y	Medium
SPBC1271.12	oxysterol binding protein	Y	n	Y	Medium
SPBC12C2.02c	Rictor homolog, Ste20	Y	n	Y	Medium
SPBC14F5.09c	adenylosuccinate lyase Ade8	n	Y	Y	Medium

SPBC14F5.13c	vacuolar membrane alkaline phosphatase	Y	n	Y	Medium
SPBC1604.08c	importin alpha	Y	n	Y	Medium
SPBC16H5.08c	Arb family ABCF2-like	Y	n	Y	Medium
SPBC1861.09	Ppk22	Y	n	Y	Medium
SPBC1921.04c	dubious	Y	n	Y	Medium
SPBC19G7.10c	topoisomerase II-associated	Y	n	Y	Medium
SPBC23E6.01c	mRNA processing factor	Y	Y	n	Medium
SPBC28F2.02	mRNA export protein Mep33	Y	n	Y	Medium
SPBC29A10.16c	cytochrome b5 (predicted)	n	Y	Y	Medium
SPBC36.07	elongator subunit Iki3	Y	n	Y	Medium
SPBC3H7.10	elongator complex subunit Elp6	Y	n	Y	Medium
SPBC428.06c	histone deacetylase complex subunit Rxt2	Y	n	Y	Medium
SPBC609.04	Caf5	Y	n	Y	Medium
SPBC646.09c	eIF3e subunit Int6	Y	n	Y	Medium
SPBC902.03	Spo7	Y	n	Y	Medium
SPBC947.08c	histone promoter control protein	n	Y	Y	Medium
SPBP8B7.22	HDEL receptor	n	Y	Y	Medium
SPCC11E10.06c	elongator complex subunit Elp4	Y	n	Y	Medium
SPCC1235.09	Set3 complex subunit Hif2	Y	n	Y	Medium
SPCC1235.11	human BRP44L ortholog	Y	Y	n	Medium
SPCC14G10.03c	Ump1	Y	n	Y	Medium
SPCC24B10.08c	Ada2	Y	Y	n	Medium
SPCC24B10.11c	THO complex subunit 7	n	Y	Y	Medium
SPCC4B3.15	medial ring protein Mid1	Y	n	Y	Medium
SPCC645.07	RhoGEF for Rho1, Rgf1	n	Y	Y	Medium
SPCC794.12c	malic enzyme, Mae2	Y	Y	n	Medium
SPAC1782.09c	Clp1/Flp1	Y	n	Y	Medium
SPAC2E1P3.04	copper amine oxidase Cao1	n	Y	Y	Medium
SPBC16A3.08c	Stm1 homolog (predicted)	Y	n	Y	Medium
SPBC18H10.09	zf-CHY type zinc finger protein	Y	n	Y	Medium
SPBC215.02	prefoldin subunit 5 (predicted)	Y	n	Y	Medium
SPBC21B10.10	40S ribosomal protein S4 (predicted)	Y	n	Y	Medium
SPBC31F10.09c	mediator complex subunit Med10	Y	n	Y	Medium
SPBC3H7.03c	2-oxoglutarate dehydrogenase	n	Y	Y	Medium
SPCC1259.01c	40S ribosomal protein S18	n	Y	Y	Medium
SPCC364.03	60S ribosomal protein L17	n	Y	Y	Medium
SPCC4B3.08	Lsk1 complex gamma subunit	Y	Y	n	Medium
SPCC584.11c	Svf1 family protein Svf1	Y	n	Y	Medium
SPAC1002.07c	N-acetyltransferase Ats1	n	n	Y	Low
SPAC1071.07c	40S ribosomal protein S15	n	Y	n	Low
SPAC110.02	cohesin-associated protein Pds5	n	Y	n	Low
SPAC1142.07c	vacuolar sorting protein Vps32	n	Y	n	Low
SPAC1142.08	fork head transcription factor Fhl1	n	Y	n	Low

SPAC11G7.02	Pub1	n	n	Y	Low
SPAC12G12.12	NST UDP-galactose transporter	n	n	Y	Low
SPAC139.01c	nuclease, XP-G family	n	Y	n	Low
SPAC1399.03	uracil permease	n	Y	n	Low
SPAC13A11.04c	Ubp8	n	n	Y	Low
SPAC13F5.03c	Gld1	n	Y	n	Low
SPAC13G6.10c	cell wall protein Asl1	n	n	Y	Low
SPAC13G7.11	mitochondrial assembly protein	n	n	Y	Low
SPAC13G7.12c	choline kinase	n	n	Y	Low
SPAC1486.01	manganese superoxide dismutase	n	n	Y	Low
SPAC14C4.16	DASH complex subunit Dad3	n	n	Y	Low
SPAC1527.01	alpha-1,3-glucan synthase Mok11	n	n	Y	Low
SPAC1565.07c	TATA-binding protein	n	n	Y	Low
SPAC15A10.16	actin interacting protein 3 homolog Bud6	n	n	Y	Low
SPAC16.03c	dihydroorotase Ura2 (predicted)	n	n	Y	Low
SPAC1610.02c	mitochondrial ribosomal protein subunit L1	n	n	Y	Low
SPAC1687.17c	Der1-like (degradation in the ER) family	n	Y	n	Low
SPAC16A10.02	transcription coactivator PC4	n	n	Y	Low
SPAC1782.05	phosphotyrosyl phosphatase activator	Y	n	n	Low
SPAC1783.07c	transcription factor Pap1/Caf3	Y	n	n	Low
SPAC17A2.11	sequence orphan	n	n	Y	Low
SPAC17A2.12	ATP-dependent DNA helicase	n	n	Y	Low
SPAC17G8.06c	dihydroxy-acid dehydratase	n	Y	n	Low
SPAC18B11.11	GTPase activating protein	n	Y	n	Low
SPAC18G6.15	EB1 family Mal3	n	Y	n	Low
SPAC1952.17c	GTPase activating protein	n	n	Y	Low
SPAC19A8.05c	Sst4	n	n	Y	Low
SPAC19G12.02c	Pms1	Y	n	n	Low
SPAC19G12.15c	Tpp1	n	n	Y	Low
SPAC19G12.16c	conserved fungal protein Adg2	n	Y	n	Low
SPAC1A6.01c	transcription coactivator	Y	n	n	Low
SPAC1A6.04c	phospholipase B homolog Plb1	n	n	Y	Low
SPAC1B3.05	Not3/5 (predicted)	n	Y	n	Low
SPAC1B3.07c	Vps28	n	n	Y	Low
SPAC1F5.07c	protoporphyrinogen oxidase	n	Y	n	Low
SPAC1F5.10	eIF4A related	Y	n	n	Low
SPAC1F7.12	YakC	n	n	Y	Low
SPAC20H4.03c	TFIIS	n	n	Y	Low
SPAC227.05	prefoldin subunit 4	n	n	Y	Low
SPAC22F3.10c	glutamate-cysteine ligase Gcs1	n	Y	n	Low
SPAC22F8.02c	PvGal biosynthesis protein Pvg5	n	n	Y	Low
SPAC22G7.11c	conserved fungal protein	n	Y	n	Low
SPAC23C11.15	Pst2	n	Y	n	Low

SPAC23G3.08c	Ubp7	n	n	Y	Low
SPAC23H3.06	pl6	n	n	Y	Low
SPAC24B11.13	hydroxymethylbilane synthase	n	Y	n	Low
SPAC24H6.07	40S ribosomal protein S9	Y	n	n	Low
SPAC25H1.02	histone demethylase Jmj1	n	n	Y	Low
SPAC26F1.10c	tyrosine phosphatase Pyp1	n	n	Y	Low
SPAC29A4.19c	Cta5	n	n	Y	Low
SPAC29E6.01	F-box protein Pof11	n	n	Y	Low
SPAC2F3.12c	human TXNDC9 ortholog	n	n	Y	Low
SPAC2F3.15	Lsk1	Y	n	n	Low
SPAC2F7.08c	SWI/SNF complex subunit Snf5	Y	n	n	Low
SPAC30.01c	ARF GEF Sec72	n	n	Y	Low
SPAC30C2.02	deoxyhypusine hydroxylase	n	n	Y	Low
SPAC31A2.06	Atp25 (predicted)	n	n	Y	Low
SPAC31A2.09c	AP-2 adaptor complex subunit Apm4	n	Y	n	Low
SPAC31G5.03	40S ribosomal protein S11	n	Y	n	Low
SPAC3C7.01c	inositol polyphosphate phosphatase	n	n	Y	Low
SPAC3C7.08c	AAA family ATPase Elf1	Y	n	n	Low
SPAC3G9.07c	histone deacetylase (class I) Hos2	Y	n	n	Low
SPAC3A11.05c	meiotic spindle pole body protein Kms1	n	n	Y	Low
SPAC3H8.02	sec14	n	n	Y	Low
SPAC3H8.07c	prefoldin subunit 3	n	n	Y	Low
SPAC4G8.13c	rz1	n	n	Y	Low
SPAC57A7.12	heat shock protein Pdr13	Y	n	n	Low
SPAC688.06c	structure-specific endonuclease subunit	Y	n	n	Low
SPAC6G10.12c	transcription factor Ace2	Y	n	n	Low
SPAC7D4.12c	DUF1212 family protein	Y	n	n	Low
SPAC821.05	translation initiation factor eIF3h (p40)	n	n	Y	Low
SPAC824.02	GPI inositol deacylase (predicted)	Y	n	n	Low
SPAC8C9.07	rRNA processing protein Fyv7 (predicted)	n	n	Y	Low
SPAC8E11.01c	beta-fructofuranosidase (predicted)	n	Y	n	Low
SPAC8E11.05c	conserved fungal protein	n	n	Y	Low
SPAC9G1.05	actin cortical patch component Aip1	n	n	Y	Low
SPAP8A3.07c	aldolase	Y	n	n	Low
SPAPYUG7.02c	Sin1	n	Y	n	Low
SPBC12C2.07c	spermidine synthase (predicted)	Y	n	n	Low
SPBC1347.01c	deoxycytidyl transferase Rev1 (predicted)	Y	n	n	Low
SPBC1347.13c	ribose methyltransferase (predicted)	Y	n	n	Low
SPBC1348.14c	hexose transporter Ght7 (predicted)	n	Y	n	Low
SPBC13E7.08c	Paf1 complex	n	n	Y	Low
SPBC146.13c	myosin type I	Y	n	n	Low
SPBC14C8.17c	SAGA complex subunit Spt8	Y	n	n	Low
SPBC1685.02c	40S ribosomal protein S12 (predicted)	n	n	Y	Low

SPBC16A3.19	Eaf7	n	Y	n	Low
SPBC16C6.09	protein O-mannosyltransferase Ogm4	Y	n	n	Low
SPBC16H5.03c	Fub2	n	n	Y	Low
SPBC16H5.06	ubiquinol-cytochrome subunit 5	n	Y	n	Low
SPBC1718.01	cullin 1 adaptor protein Pop1	n	n	Y	Low
SPBC1734.12c	Alg12	n	n	Y	Low
SPBC18H10.10c	Saf4	Y	n	n	Low
SPBC18H10.14	40S ribosomal protein S16 (predicted)	Y	n	n	Low
SPBC1A4.09	pseudouridine synthase (predicted)	n	n	Y	Low
SPBC1D7.03	cyclin Clg1 (predicted)	n	n	Y	Low
SPBC21.05c	Ras1-Scd pathway protein Ral2	Y	n	n	Low
SPBC21C3.13	40S ribosomal protein S19 (predicted)	n	Y	n	Low
SPBC23E6.08	Sat1	Y	n	n	Low
SPBC23G7.08c	Rho-type GTPase activating protein Rga7	n	n	Y	Low
SPBC25D12.02c	nucleolar protein Dnt1	Y	n	n	Low
SPBC25H2.15	Tsr4 homolog 1	n	Y	n	Low
SPBC27.08c	sulfate adenylyltransferase	n	n	Y	Low
SPBC27B12.11c	transcription factor (predicted)	Y	n	n	Low
SPBC2G2.01c	pantothenate transporter Liz1	n	n	Y	Low
SPBC2G2.03c	translocon beta subunit Sbh1 (predicted)	Y	n	n	Low
SPBC2G5.06c	sulfide-quinone oxidoreductase	n	n	Y	Low
SPBC317.01	Pvg4	n	n	Y	Low
SPBC31F10.10c	zf-MYND type zinc finger protein	Y	n	n	Low
SPBC32F12.08c	DASH complex subunit Duo1	n	n	Y	Low
SPBC336.03	Efc25	n	n	Y	Low
SPBC336.14c	Ppk26	n	n	Y	Low
SPBC359.06	adducin	n	n	Y	Low
SPBC36.06c	farnesyl pyrophosphate synthetase	n	n	Y	Low
SPBC365.13c	Ran GTPase binding protein Hba1	n	n	Y	Low
SPBC3B8.10c	Nem1	n	n	Y	Low
SPBC530.06c	eIF3 alpha subunit (p135)	n	n	Y	Low
SPBC685.06	40S ribosomal protein S0A (p40)	Y	n	n	Low
SPBC725.09c	BAR adaptor protein Hob3	Y	n	n	Low
SPBC776.17	rRNA processing protein Rrp7 (predicted)	n	n	Y	Low
SPBC800.04c	60S ribosomal protein L37a (predicted)	n	Y	n	Low
SPBC800.07c	Tsf1	n	Y	n	Low
SPBP22H7.08	40S ribosomal protein S10 (predicted)	n	Y	n	Low
SPBP35G2.07	acetolactate synthase catalytic subunit	n	n	Y	Low
SPBPB2B2.10c	Gal7	n	n	Y	Low
SPCC1442.02	kinetochore associated	n	n	Y	Low
SPCC14G10.04	sequence orphan	n	n	Y	Low
SPCC1840.10	Lsm8	n	n	Y	Low

SPCC188.07	telomere maintenance protein Ccq1	Y	n	n	Low
SPCC1906.02c	CUE domain protein Cue3	Y	n	n	Low
SPCC23B6.01c	oxysterol binding protein	n	Y	n	Low
SPCC306.09c	adenylyl cyclase-associated protein Cap1	Y	n	n	Low
SPCC31H12.08c	Ccr4	n	Y	n	Low
SPCC320.03	transcription factor (predicted)	n	n	Y	Low
SPCC576.12c	FANCM-MHF complex subunit Mhf2	n	n	Y	Low
SPCC794.07	Lat1	n	n	Y	Low
SPCC830.06	calcineurin regulatory subunit (predicted)	n	n	Y	Low
SPCC895.05	formin For3	n	n	Y	Low
SPAC13C5.01c	20S proteasome component alpha 3 (predicted)	n	n	Y	Low
SPAC1486.08	Cox16	n	n	Y	Low
SPAC14C4.06c	poly(A) binding protein Nab2 (predicted)	n	n	Y	Low
SPAC1556.01c	DNA repair protein Rad50	n	n	Y	Low
SPAC17D4.04	tRNA methyltransferase	n	n	Y	Low
SPAC1805.07c	DASH complex subunit Dad2	n	n	Y	Low
SPAC19B12.04	40S ribosomal protein S30 (predicted)	n	n	Y	Low
SPAC20G4.07c	C-24(28) sterol reductase Sts1	n	Y	n	Low
SPAC22E12.19	Set3 complex subunit Snt1	Y	n	n	Low
SPAC23C11.04c	DNA kinase/phosphatase Pnk1	n	n	Y	Low
SPAC23C4.12	serine/threonine protein kinase Hhp2	n	n	Y	Low
SPAC23G3.03	ornithine N5 monooxygenase (predicted)	n	n	Y	Low
SPAC23H3.09c	threonine aldolase Gly1 (predicted)	Y	n	n	Low
SPAC25B8.05	tRNA-pseudouridine synthase (predicted)	Y	n	n	Low
SPAC2F7.04	mediator complex subunit Pmc2/Med1	n	n	Y	Low
SPAC3A11.08	cullin 4	n	n	Y	Low
SPAC3A11.13	prefoldin subunit 6 (predicted)	n	n	Y	Low
SPAC3C7.06c	Pit1	n	n	Y	Low
SPAC4D7.10c	SAGA complex subunit Spt20 (predicted)	n	n	Y	Low
SPAC513.03	M-factor precursor Mfm2	n	Y	n	Low
SPBC1921.07c	SAGA complex subunit Sgf29 (predicted)	Y	n	n	Low
SPBC29A3.21	sequence orphan	Y	n	n	Low
SPBC3H7.05c	sequence orphan	Y	n	n	Low
SPBC725.02	Mpr1	n	n	Y	Low
SPBC839.04	60S ribosomal protein L8	n	n	Y	Low
SPCC1450.05c	mediator complex subunit Med19/Rox3	n	n	Y	Low
SPCC364.05	GTPase regulator Vps3 (predicted)	n	Y	n	Low
SPCC550.12	actin-like protein Arp6	n	n	Y	Low
SPCC63.02c	alpha-amylase homolog Aah3	n	n	Y	Low
SPCPB16A4.04c	Trm8	n	n	Y	Low

Appendix B: CLUSTAL O (1.2.4) multiple sequence alignment

```

FLO8_BUDDING_YEAST -----
ADN2_FISSION_YEAST -----SPCCMADPGLRSGVG
Y53F4B.5_WORM -----MDPQYPDE-----SF-----LFQPRGGPPPG---G-P
SAM-10_WORM -----
SSDP_DROSOPHILA -----
Si:ch211-130m23.3_ZEBRAFISH -----
SSBP2_ZEBRAFISH -----
SSBP42_RAT MQGLTSEPATEPRRAPQWEAGTVPPGERRRLAQSLSQKVEGSEASPACWPSPGN---GIG
SSBP2_HUMAN -----
SSBP2_MOUSE -----
SSBP4_HUMAN -----
SSBP4_MOUSE -----
SSBP4_RAT -----
SSBP3b_ZEBRAFISH -----
SSBP3a_ZEBRAFISH -----
SSBP3_HUMAN -----
SSBP3_MOUSE -----
SSBP3_RAT -----
Zgc:110158_ZEBRAFISH -----
SSBP4_ZEBRAFISH -----

```

```

FLO8_BUDDING_YEAST -----TAENSDLKEKMCKNTLNEYIFDF--LTKSSLKNTAAFAQDAH-
ADN2_FISSION_YEAST LPSQQGQKHDLDQKQKPHVNNADRTTQSLNLSYIYDY--LIKDYCEAARAFGREA--
Y53F4B.5_WORM QDVPLQS-MPPQAIQQQQSLASEMIARDRLEHIVKHVKYKYPFNCPCRRLFASQKEVDG
SAM-10_WORM -----MPPQVIQQQQSLASEMTARDRLTSYIYDY--LQQ-----TG-ASK----
SSDP_DROSOPHILA -----MYGK-SKTSAVPSDAQAREKLALYVYDY--LLH-----VG-AQK----
Si:ch211-130m23.3_ZEBRAFISH -----MYAK-GK-SSVPSDSQAREKLALYVYDY--LLH-----VG-AQK----
SSBP2_ZEBRAFISH -----MYAK-GKSNVPSDSQAREKLALYVYDY--LLH-----VG-AQK----
SSBP42_RAT ATPQTGG-MRST-A-GNGAGSLAGEERERRLALYVYDY--LLH-----VG-AQK----
SSBP2_HUMAN -----MYGK-GK-SNSAVPSDSQAREKLALYVYDY--LLH-----VG-AQK----
SSBP2_MOUSE -----MYGK-GK-SNSAVPSDSQAREKLALYVYDY--LLH-----VG-AQK----
SSBP4_HUMAN -----MYAGKGGKSAVPSDSQAREKLALYVYDY--LLH-----IG-AQK----
SSBP4_MOUSE -----MYGKASKG-CAPSDGQAREKLALYVYDY--LLH-----VG-AQK----
SSBP4_RAT -----MYGKASKG-CAPSDGQAREKLALYVYDY--LLH-----VG-AQK----
SSBP3b_ZEBRAFISH -----MFPK-GKSSVPSDSQAREKLALYVYDY--LLH-----IG-AQK----
SSBP3a_ZEBRAFISH -----MFAK-GKGTAVPSDSQAREKLALYVYDY--LLH-----VG-AQK----
SSBP3_HUMAN -----MFAK-GKGSVPSDSQAREKLALYVYDY--LLH-----VG-AQK----
SSBP3_MOUSE -----MFAK-GKGSVPSDSQAREKLALYVYDY--LLH-----VG-AQK----
SSBP3_RAT -----MFAK-GKGSVPSDSQAREKLALYVYDY--LLH-----VG-AQK----
Zgc:110158_ZEBRAFISH -----MYAK-GKGA VPSDSQAREKLALYVYDY--LLH-----VG-AQK----
SSBP4_ZEBRAFISH -----MYAK-GKGA VPSDSQAREKLALYVYDY--LLH-----VG-AQK----

```

```

FLO8_BUDDING_YEAST ----LD-----RDKGQNPVD-----GPKSKENNGNQNTF-----
ADN2_FISSION_YEAST QVQTLVRSQEEFNLSLAKRHKRMSVPAVKHEGHSNNESSDENMNVNGLDSESSSAPPP
Y53F4B.5_WORM HQENRHAE-----LDWKSVEPFAEEEQ-IYRRS-----MNMVNGNLDSESSSAPPP
SAM-10_WORM TAETFKEE-----VLSTNPAA-----GLA
SSDP_DROSOPHILA AAQTFLSE-----IRWEK-----
Si:ch211-130m23.3_ZEBRAFISH SAQTFLSE-----IRWEK-----
SSBP2_ZEBRAFISH SAQTFLSE-----IRWEK-----
SSBP42_RAT SAQTFLSE-----IRWEK-----
SSBP2_HUMAN SAQTFLSE-----IRWEK-----
SSBP2_MOUSE SAQTFLSE-----IRWEK-----
SSBP4_HUMAN SAQTFLSE-----IRWEK-----
SSBP4_MOUSE SAQTFLSE-----IRWEK-----
SSBP4_RAT SAQTFLSE-----IRWEK-----
SSBP3b_ZEBRAFISH SAQTFLSE-----IRWEK-----
SSBP3a_ZEBRAFISH SAQTFLSE-----IRWEK-----
SSBP3_HUMAN SAQTFLSE-----IRWEK-----
SSBP3_MOUSE SAQTFLSE-----IRWEK-----
SSBP3_RAT SAQTFLSE-----IRWEK-----
Zgc:110158_ZEBRAFISH SAQTFLSE-----IRWEK-----
SSBP4_ZEBRAFISH SAQTFLSE-----IRWEK-----

```

```

FLO8_BUDDING_YEAST --SKVVDTPQGFLYEW*QIFWDFINTSSSRGGSEFAQQYYQLVQLQEQEQIYRSLAVH-
ADN2_FISSION_YEAST PPILPIDSAGGFLEWVWVFDIYNARRGQSEPEAKAYMSHIS-NLRK---KSRNLNLQE
Y53F4B.5_WORM KRNIKNGKPEGYQKSSVD-----KDTKMTL-SH-----
SAM-10_WORM AANSTKLSDKSFLEWVWVFDIYNARRGQSEPEAKAYMSHIS-NLRK---KSRNLNLQE
SSDP_DROSOPHILA --NITLGEPPGFLHWTWVWVFDIYNARRGQSEPEAKAYMSHIS-NLRK---KSRNLNLQE
Si:ch211-130m23.3_ZEBRAFISH --NITLGEPPGFLHWTWVWVFDIYNARRGQSEPEAKAYMSHIS-NLRK---KSRNLNLQE
SSBP2_ZEBRAFISH --NITLGEPPGFLHWTWVWVFDIYNARRGQSEPEAKAYMSHIS-NLRK---KSRNLNLQE
SSBP42_RAT --NITLGEPPGFLHWTWVWVFDIYNARRGQSEPEAKAYMSHIS-NLRK---KSRNLNLQE
SSBP2_HUMAN --NITLGEPPGFLHWTWVWVFDIYNARRGQSEPEAKAYMSHIS-NLRK---KSRNLNLQE
SSBP2_MOUSE --NITLGEPPGFLHWTWVWVFDIYNARRGQSEPEAKAYMSHIS-NLRK---KSRNLNLQE
SSBP4_HUMAN --NITLGEPPGFLHWTWVWVFDIYNARRGQSEPEAKAYMSHIS-NLRK---KSRNLNLQE

```

```

SSBP4_MOUSE --NITLGEPPGFLHSWWCVFWDLYCAAPDRREAC-EH--SSEAK-VFQD---YSAA----
SSBP4_RAT --NITLGEPPGFLHSWWCVFWDLYCAAPDRREAC-EH--SSEAK-VFQD---YSAA----
SSBP3b_ZEBRAFISH --NITLGDPPPGLHSWWCVFWDLYCAAPERRDTC-EH--SSEAK-AFHD---YSAA----
SSBP3a_ZEBRAFISH --NITLGEPPGFLHSWWCVFWDLYCAAPERRDTC-DH--SSEAK-AFHD---YSAA----
SSBP3_HUMAN --NITLGEPPGFLHSWWCVFWDLYCAAPERRDTC-EH--SSEAK-AFHD---YSAA----
SSBP3_MOUSE --NITLGEPPGFLHSWWCVFWDLYCAAPERRDTC-EH--SSEAK-AFHD---YSAA----
SSBP3_RAT --NITLGEPPGFLHSWWCVFWDLYCAAPERRDTC-EH--SSEAK-AFHD---YSAA----
Zgc:110158_ZEBRAFISH --NITLGEPPGFLHSWWCVFWDLYCAAPDRRETC-EH--SSEAK-AFHD---YSAA----
SSBP4_ZEBRAFISH --NITLGEPPGFLHSWWCVFWDLYCAAPDRRETC-EH--SSEAK-AFHD---YSAA----

```

..

```

FLO8_BUDDING_YEAST -AARLQHDAAERREYSNEDIDPMHLAAMMLGNPMAPAV--QMRNVNMNPI-----PIP
ADN2_FISSION_YEAST IQKNSLHTGNTSHPYANASFPHDPA-----NAMGQQIDSSQFHQAGGLNDRNQH
Y53F4B.5_WORM -----
SAM-10_WORM -----MP-----PGMNGHFAPPMMGEMM-GGHPGAFGGRFAPGRMPPG-----
SSDP_DROSOPHILA --SS-----GYGVNGIGPG---GPHNAGGPAPSP-----LGQMPGGGDG-----GP
Si:ch211-130m23.3_ZEBRAFISH ---A-----TQSPV-----IGS-PPG-DG-----
SSBP2_ZEBRAFISH ---A-----APSPV-----LGNMQPG-EG-----
SSBP42_RAT ---A-----APSPV-----LGNMPPG-DG-----
SSBP2_HUMAN ---A-----APSPV-----LGNIPPG-DG-----
SSBP2_MOUSE ---A-----APSPV-----LGNMPPG-DG-----
SSBP4_HUMAN ---A-----APSPV-----MGSMAPG-DT-----
SSBP4_MOUSE ---A-----APSPV-----MGAMTNP-DA-----
SSBP4_RAT ---AA-----APSPV-----MGTILAPN-DA-----
SSBP3b_ZEBRAFISH ---A-----APSPV-----LGNMPPG-DG-----
SSBP3a_ZEBRAFISH ---A-----APSPV-----LGNLPPG-DG-----
SSBP3_HUMAN ---A-----APSPV-----LGNIPPN-DG-----
SSBP3_MOUSE ---A-----APSPV-----LGNIPPN-DG-----
SSBP3_RAT ---A-----APSPV-----LGNIPPN-DG-----
Zgc:110158_ZEBRAFISH ---A-----APSPV-----MGNMPPN-DG-----
SSBP4_ZEBRAFISH ---A-----APSPV-----MGNMPPN-DG-----

```

```

FLO8_BUDDING_YEAST MVGNPIVNNFSIPPYNNANPTTGATAVAPTAPPSGDFTNVGPQTQ-----NRS-QNVT
ADN2_FISSION_YEAST LMRQAMLNNQSRRET-----FPPTAAQLQLKQLHYRQLQSVQQQKQHQKQKKT
Y53F4B.5_WORM -----
SAM-10_WORM AMAP-----GG-----MPPGAFPMFPPD---P-----R-----
SSDP_DROSOPHILA MGPG-----GP-----MGNFFFNSTMRPSP---T-HASS
Si:ch211-130m23.3_ZEBRAFISH -MP-----GP-----LPPGFFQ-----
SSBP2_ZEBRAFISH -MPV-----GP-----VPPGFFQ-----
SSBP42_RAT -MPV-----GP-----VPPGFFQ-----
SSBP2_HUMAN -MPV-----GP-----VPPGFFQ-----
SSBP2_MOUSE -MPV-----GP-----VPPGFFQ-----
SSBP4_HUMAN -MAA-----GS-----MAAGFFQGGPPGSQPSP-----H-----
SSBP4_MOUSE -MAA-----GP-----VAPGFFQ-----
SSBP4_RAT -MAA-----GP-----VAPGFFQ-----
SSBP3b_ZEBRAFISH -MPG-----GP-----MPPGFFQGGPPGSQASP-----H-APP
SSBP3a_ZEBRAFISH -MPG-----GP-----IPPGFFQGGPPGSQPSP-----H-AQLP
SSBP3_HUMAN -MPG-----GP-----IPPGFFQGGPPGSQPSP-----H-AQPP
SSBP3_MOUSE -MPG-----GP-----IPPGFFQGGPPGSQPSP-----H-AQPP
SSBP3_RAT -MPG-----GP-----IPPGFFQ-----
Zgc:110158_ZEBRAFISH -MPG-----GP-----MPPGFFQGGPPGSQPSP-----H-AQPP
SSBP4_ZEBRAFISH -MPG-----GP-----MPPGFFQGGPPGSQPSP-----H-AQPP

```

```

FLO8_BUDDING_YEAST GWPVYNYPMQPTTENPVGNPCNNNTTNNNTNNSPVNQF---KSLKTMHSTDKPNNVPTS
ADN2_FISSION_YEAST PQSGSTPQMONTTSQPTT-----HDTHPKQQGPISDFRSIPSSPK-----
Y53F4B.5_WORM -----L-QRMA-----PNQGM-RMPPPPV-----G
SAM-10_WORM PQPPPS-QMMPGQPPFMG-----GPRYPGGPRPGVR-MQGMGNEFNPPG
SSDP_DROSOPHILA -----QFM-----SPRYPGGPRGSLR-IPNQAL-G---PGN
Si:ch211-130m23.3_ZEBRAFISH -----PFM-----SSRYPGGPRPALR-IPNQAL-AGVPGN
SSBP2_ZEBRAFISH -----PFM-----SPRYPGGPRPPLR-IPNQAL-GGVPGS
SSBP42_RAT -----PFM-----SPRYPGGPRPPLR-IPNQAL-GGVPGS
SSBP2_HUMAN -----PFM-----SPRYPGGPRPPLR-IPNQAL-GGVPGS
SSBP2_MOUSE --NPNA-PMMGPHGQPFM-----SPRFPGGPRPPLR-MPSQPP-AGLPGS
SSBP4_HUMAN -----PFM-----SPRFPGGARFILR-MPGQPP-VGLPGS
SSBP4_MOUSE -----PFI-----SPRFPGGARFILR-MPGQPP-VGLPGS
SSBP4_RAT P-----N-SMMGPHGQPFM-----SPRFGGGPRPPIR-MGNQPP-GGVPA
SSBP3b_ZEBRAFISH PN---A-NMMAAHGQPFM-----SPRYAGGPRPPIR-MGNQPP-G---G
SSBP3a_ZEBRAFISH PHNPS--SMMGPHSQPFFM-----SPRYAGGPRPPIR-MGNQPP-GGVPGT
SSBP3_HUMAN PHNPS--SMMGPHSQPFFM-----SPRYAGGPRPPIR-MGNQPP-GGVPGT
SSBP3_MOUSE -----PFM-----SPRYAGGPRPPIR-MGNQPP-GGVPGT
SSBP3_RAT PHNTSN-PMMGPHGQPFM-----SPRYPGGPRPPLR-MPNQPP-VGVPGS
Zgc:110158_ZEBRAFISH PHNPNN-PMMGPHGQPFM-----SPRYPGGPRPPLR-MPNQPP-VGVPGS
SSBP4_ZEBRAFISH

```

```

FLO8_BUDDING_YEAST KSTRSRSA--TSKAKGKVA-GLVAKRRRNNTATVSAGSTNACSPNITTPGTTSEPM
ADN2_FISSION_YEAST -----TEGAPSN---AQFRP---SLPATNGSVQSNFLYDTGLNGQYV
Y53F4B.5_WORM -----
SAM-10_WORM QPFFGAVGMPRPVPGAPMDMSGMRQDFD----MGGPPPGGGAQFPFGASGSGMMPNG

```

```

SSDP_DROSOPHILA          QPMMPNSMDPTREPGGGM---GPMNPRMNP--PRGPGMGPMGY-----GGPGGMRG-
Si:ch211-130m23.3_ZEBRAFISH QPLLPSGMDPT-RQPGHPSLSGPMQRMTP--PRGMVPIGP--Q-----NYGGGMRP-
SSBP2_ZEBRAFISH          QPLI----DPS-RQQGHPNMAGAMQRMTP--PRGMVPLGP--Q-----YGGGMRP-
SSBP42_RAT                QPLLPSGMDPT-RQQGHPNMGGGPMQRMTP--PRGMVPLGP--QSDPWLSLQNYGGAMRP-
SSBP2_HUMAN              QPLLPSGMDPT-RQQGHPNMGGGPMQRMTP--PRGMVPLGP--Q-----NYGGAMRP-
SSBP2_MOUSE              QPLLPSGMDPT-RQQGHPNMGGGPMQRMTP--PRGMVPLGP--Q-----NYGGAMRP-
SSBP4_HUMAN              QPLLPGAMEPSPRAQGHPSMGGGPMQRVTP--PRGMASVGP--Q-----SYGGGMRP-
SSBP4_MOUSE              QPLIPAAMDPSPRVQGHPSLGGGPMQRVTP--PRGMASVGP--Q-----GYGTGMRP-
SSBP4_RAT                QHLIPGAMDPSRAQGHPSLGGGPMQRVTP--PRGMASVGP--Q-----GFGTGMRP-
SSBP3b_ZEBRAFISH        QPMLPNM-----DPRLQGPMQRMNV--PRGMGPMGPGPQ-----FGGGGMRP-
SSBP3a_ZEBRAFISH        QPLPNMMDPT-RPTGHPNLA-SMQRMNA--PRGMGPMGPGPQSDPWLSLQNYGGGMRP-
SSBP3_HUMAN              QPLLNSMDPT-RQQGHPNMGGGSMQRMNP--PRGMGPMGPGPQ-----NYSGGMRP-
SSBP3_MOUSE              QPLLNSMDPT-RQQGHPNMGGGSMQRMNP--PRGMGPMGPGPQ-----NYSGGMRP-
SSBP3_RAT                QPLPNMMDPT-RPTGHPNLA-SMQRMNA--PRGMGPMGPGPQ-----NYSGGMRP-
Zgc:110158_ZEBRAFISH    QPLLNSLDPT-RPQGHPNMGGGPM-RMNP--PRGMGGM--GPQ-----NYG-GMRP-
SSBP4_ZEBRAFISH        QPLLNSLDPT-RPQGHPNMGGGPM-RMNP--PRGMGGM--GPQ-----NYGGGMRP-

```

```

FLO8_BUDDING_YEAST      VGSRVNKTPRSDIATNFRNQAIIFGEEDIYSNSKSSPSLD----GASPSALASKOPTKV
ADN2_FISSION_YEAST      VQN-----SAQPLLHEINFASN--RNPHLKQG--GAVPSSTLPQQQKSL
Y53F4B.5_WORM          -----
SAM-10_WORM            AH-----PHMSLNSPSMGVPPADMP-----
SSDP_DROSOPHILA        -----PA--P-GGGMPPMGMG-----
Si:ch211-130m23.3_ZEBRAFISH -----PLNALV-GP-GMPGINMG-----
SSBP2_ZEBRAFISH        -----PLNALG-GP-P--MNMG-----
SSBP42_RAT              -----PLNALG-GP-GMPGMNMG-----
SSBP2_HUMAN            -----PLNALG-GP-GMPGMNMG-----
SSBP2_MOUSE            -----PLNALG-GP-GMPGMNMG-----
SSBP4_HUMAN            -----PPNSLA-GP-GLPAMNMG-----
SSBP4_MOUSE            -----PPNSLA-TSQVLPMSNMG-----
SSBP4_RAT              -----PPNSLA-TSQILPSMNMG-----
SSBP3b_ZEBRAFISH      -----PHNSM--GP-GMPGVNMG-----
SSBP3a_ZEBRAFISH      -----PNS--M-GP-GMPGVNMV-----
SSBP3_HUMAN            -----PPNSLG--P-AMPGINMG-----
SSBP3_MOUSE            -----PPNSLG--P-AMPGINMG-----
SSBP3_RAT              -----PPNSLG--P-AMPGINMG-----
Zgc:110158_ZEBRAFISH  -----PPNSLG-GP-GMPGMNMG-----
SSBP4_ZEBRAFISH        -----PPNSLG-GP-GMPGMNMG-----

```

```

FLO8_BUDDING_YEAST      RKNTKASTSAFFVESTNKLGGNSVV-TGKKRSPNTRVRRKSTPSVILNADATKDENN
ADN2_FISSION_YEAST      DKP----KPAQ--QPSTGQFSGNQMNQYGFNSN-----PYSQN
Y53F4B.5_WORM          -----
SAM-10_WORM            -----PFMGM-----
SSDP_DROSOPHILA        -----GAGGR-----
Si:ch211-130m23.3_ZEBRAFISH -----PAGGR-----
SSBP2_ZEBRAFISH        -----P-GGR-----
SSBP42_RAT              -----PGGGR-----
SSBP2_HUMAN            -----PGGGR-----
SSBP2_MOUSE            -----PGGGR-----
SSBP4_HUMAN            -----PGVRG-----
SSBP4_MOUSE            -----PGVRG-----
SSBP4_RAT              -----PGVRG-----
SSBP3b_ZEBRAFISH      -----PGNGR-----
SSBP3a_ZEBRAFISH      -----AGAGR-----
SSBP3_HUMAN            -----PGAGR-----
SSBP3_MOUSE            -----PGAGR-----
SSBP3_RAT              -----PGAGR-----
Zgc:110158_ZEBRAFISH  -----PGGRG-----
SSBP4_ZEBRAFISH        -----PGGRG-----

```

```

FLO8_BUDDING_YEAST      MLRTFSNTIAPNIHSAPPTKTANSLP-----F--PGINLGSFNKPAVSSPLSSV
ADN2_FISSION_YEAST      MLYNFNGNANPRLNPAKKNYMEELKLEQQNKKRLLLVSQEKERKGYT---SASPDRPL
Y53F4B.5_WORM          -----
SAM-10_WORM            -----PPMPF-----TSSSAMPFG---MSSDHQPM
SSDP_DROSOPHILA        -----PPQWQPN-----ASAPLNAYS---SSSP---
Si:ch211-130m23.3_ZEBRAFISH -----P-WPNP-----PNNNSIPYS---SASP---
SSBP2_ZEBRAFISH        -----P-WPNP-----PNSNSIPYS---SASP---
SSBP42_RAT              -----P-WPNP-----TNANSIPYS---SASP---
SSBP2_HUMAN            -----P-WPNP-----TNANSIPYS---SASP---
SSBP2_MOUSE            -----P-WPNP-----TNANSIPYS---SASP---
SSBP4_HUMAN            -----P-WASP-----S-GNSIPYS---SSSP---
SSBP4_MOUSE            -----P-WASP-----S-GNSIPYS---SSSP---
SSBP4_RAT              -----P-WASP-----S-GNSIPYS---SSSP---
SSBP3b_ZEBRAFISH      -----PP-WPNP-----NA-NMPPYS---SPSP---
SSBP3a_ZEBRAFISH      -----P-WPNP-----NNGNTISYS---SSSP---
SSBP3_HUMAN            -----P-WPNP-----NSANSIPYS---SSSP---
SSBP3_MOUSE            -----P-WPNP-----NSANSIPYS---SSSP---
SSBP3_RAT              -----P-WPNP-----NSANSIPYS---SSSP---
Zgc:110158_ZEBRAFISH  -----P-WPNP-----NA-NSIAYS---SSSP---

```

```

SSBP4_ZEBRAFISH -----P-WPNP-----NP-NSIAYS---SSSP----

FLO8_BUDDING_YEAST      TESCFDPESGKIAGKNGPKRAVNSKVSASSPLSIATPRSGDAQKQRSSKVPGNVVIKPP-
ADN2_FISSION_YEAST      SQTITESSVAKT-----KSTTPKSTDTPTTEA--TSPVKVSTKNSN
Y53F4B.5_WORM
SAM-10_WORM              SAGPAAAAAPGATT--AGGPGTIPM-----IGSVPGPGSVPVQA-TTSVGSV-----
SSDP_DROSOPHILA         --GNYGPGSNG---PPGPGTIPM-----PSPQD-----NTQGGFV-----
Si:ch211-130m23.3_ZEBRAFISH --GSYSGPPAG---GGPPGTIPM-----PSPAE-----SNNS-----
SSBP2_ZEBRAFISH         --GSYVGPPEG---GGPPGTIPM-----PSPAD-----STNS-----
SSBP42_RAT              --GNYVGPPEG---GGPPGTIPM-----PSPAD-----STNS-----
SSBP2_HUMAN             --GNYVGPPEG---GGPPGTIPM-----PSPAD-----STNS-----
SSBP2_MOUSE            --GNYVGPPEG---GGPPGTIPM-----PSPAD-----STNS-----
SSBP4_HUMAN             --GSYTGPPGG---GGPPGTIPM-----PSPGD-----STNS-----
SSBP4_MOUSE            --GSYSGPAGV---GGAPGTIPM-----PSPGD-----STNS-----
SSBP4_RAT              --GSYSGPTGG---GGAPGTIPM-----PSPGD-----STNS-----
SSBP3b_ZEBRAFISH       --GAYGGPQGG---GPPGTIPM-----PSPAD-----SNNS-----
SSBP3a_ZEBRAFISH       --GTYVGPPEGAGGGGCPGTIPM-----PSPAD-----STNS-----
SSBP3_HUMAN            --GTYVGPPEG---GGPPGTIPM-----PSPAD-----STNS-----
SSBP3_MOUSE            --GTYVGPPEG---GGPPGTIPM-----PSPAD-----STNS-----
SSBP3_RAT              --GTYVGPPEG---GGPPGTIPM-----PSPAD-----STNS-----
Zgc:110158_ZEBRAFISH   --GNYVGPPEG---GGPPGTIPM-----PSPGD-----STNS-----
SSBP4_ZEBRAFISH       --GNYVGPPEG---GGPPGTIPM-----PSPGD-----STNS-----

FLO8_BUDDING_YEAST      -----HGFSTTNLNI TLKNSKI ITS-----QNNTVSQELPNGNILEAQVGNDSR
ADN2_FISSION_YEAST      TTENLNGINESNMPMLQNLPLRTSGDHP SNYSNLIENSSTSDTNADNGMDV-----
Y53F4B.5_WORM
SAM-10_WORM              -----GTPSSIGQQLHQPKQEI TTNGE---EIMKT---EALTP TGGGGGGG---
SSDP_DROSOPHILA         -----GGPGDSMYALMKP-----EFPMGG---GPDGGGGGGGGGG---
Si:ch211-130m23.3_ZEBRAFISH -----SDNLYMIS---VPPNGTR-PNFPLGS---GADGPIGS--MAG-----
SSBP2_ZEBRAFISH         -----GENMYTMINA---VPPGANRQ-NFPLGA---GGEGPLGG--LAG-----
SSBP42_RAT              -----GDNMYTLMNA---VPPGNRPNQFPMGP---GSDGPMGG--LGG-----
SSBP2_HUMAN             -----GDNMYTLMNA---VPPGNRPN-FPMGP---GSDGPMGG--LGG-----
SSBP2_MOUSE            -----GDNMYTLMNA---VPPGNRPN-FPMGP---GSDGPMGG--LGG-----
SSBP4_HUMAN             -----SENMYTIMNP---IGQGAGR-ANFPLGP---GPEGPMAA--MSA-----
SSBP4_MOUSE            -----SENMYTIMNP---IGPGAGR-ANFPLGP---SPEGPMAS--MST-----
SSBP4_RAT              -----SENMYTIMNP---IGPGAGR-ANFPLGP---SPEGPMAS--MST-----
SSBP3b_ZEBRAFISH       -----SENLYTMINS---G---GGGR-NNFPIGP---GSEGPLGA--MAG-----
SSBP3a_ZEBRAFISH       -----GENLYTLINS---VPPGGNR-SSFMTGP---GSDGPMG---G-----
SSBP3_HUMAN            -----SDNIYTMINP---VPPGGR-SNFFMGP---GSDGPMGG--MGG-----
SSBP3_MOUSE            -----SDNIYTMINP---VPPGGR-SNFFMGP---GSDGPMGG--MGG-----
SSBP3_RAT              -----SDNIYTMINP---VPPGGR-SNFFMGP---GSDGPMGG--MGG-----
Zgc:110158_ZEBRAFISH   -----SENIYTMNPN---IGPGNR-PNFPMGP---GPDGPMGG--MGG-----
SSBP4_ZEBRAFISH       -----SENIYTMNPN---IGPGNR-PNFPMGP---GPDGPMGG--MGA-----

FLO8_BUDDING_YEAST      SSKGNRNTLSTPEEKKPSSNNQ-----GYDFDALKNSSSLLFPNQAYASNNRTPNENSNV
ADN2_FISSION_YEAST      --MGNW--QLQQTHSSRPTPNASS---PLDVRSKQK-----P---SSANSNAPT PAPT V
Y53F4B.5_WORM
SAM-10_WORM              --VPPP--PPA---ATAAVSMNGGGPGSAPGSAHSVNNN---VNPPTPGSNPLSNPMSNPPL
SSDP_DROSOPHILA         --MGPM--GGG--PNSMGFVLNGGG--GPDGSGLDGMK-----NSP----A
Si:ch211-130m23.3_ZEBRAFISH --MEP-----HH---MNGSL-G--SGDIESLKP-----SSPGNLS--M
SSBP2_ZEBRAFISH         --LEP-----HH---MNGSL-G--SADMDSMPK-----NSPGNLS--M
SSBP42_RAT              --MES-----HH---MNGSL-G--SGDMSISK-----NSPNNMS--L
SSBP2_HUMAN             --MES-----HH---MNGSL-G--SGDMSISK-----NSPNNMS--L
SSBP2_MOUSE            --MES-----HH---MNGSL-G--SGDMSISK-----NSPNNMS--L
SSBP4_HUMAN             --MEP-----HH---VNGSL-G--SGDMDGLPK-----NSPGAVAGL
SSBP4_MOUSE            --MEP-----HH---VNGSL-G--SGDMDGLPK-----NSPGAVGGL
SSBP4_RAT              --MEP-----HH---VNGSL-G--SGDMDGLPK-----NSPGAVGGL
SSBP3b_ZEBRAFISH       --MDP-----MH---MNG--G--SGDLGLPK-----NSPNNMSGM
SSBP3a_ZEBRAFISH       --LEP-----HH---MNGSL-G--SGDIDGLTK-----NSPNNLSGL
SSBP3_HUMAN            --MEP-----HH---MNGSL-G--SGDIDGLPK-----NSPNNISGI
SSBP3_MOUSE            --MEP-----HH---MNGSL-G--SGDIDGLPK-----NSPNNISGI
SSBP3_RAT              --MEP-----HH---MNGSL-G--SGDINGLPK-----NSPNNISGI
Zgc:110158_ZEBRAFISH   --MEP-----HH---MNGSL-G--SGDMDGLPK-----NSPNNMAGM
SSBP4_ZEBRAFISH       --MEP-----HH---MNGSL-G--SGDMDGLPK-----NSPNNMAGM

FLO8_BUDDING_YEAST      ADETSASTNSGDNDNTLIQSSNVGTTLGPQQT-----
ADN2_FISSION_YEAST      NTT--NP-ESSTNE-----ATSVGPALEPSQGANVHKS DSELNQNQSGKSNPDTSATP
Y53F4B.5_WORM
SAM-10_WORM              SSG--PPPPGSNDA-----FGKDDN---
SSDP_DROSOPHILA         NGG--PGTPREDSG-----SGMGDYNLGGFGGP-----GENDQTES---
Si:ch211-130m23.3_ZEBRAFISH NNQ--PGTPRDDGE-----M--SGNFLNPFQSE-----SYSPNMT---
SSBP2_ZEBRAFISH         SNQ--PGTPRDDGE-----M--AGNFLNPFQSE-----SYSPNMT---
SSBP42_RAT              SNQ--PGTPRDDGE-----M--GGNFLNPFQSE-----SYSPSMT---
SSBP2_HUMAN             SNQ--PGTPRDDGE-----M--GGNFLNPFQSE-----SYSPSMT---
SSBP2_MOUSE            SNQ--PGTPRDDGE-----M--GGNFLNPFQSE-----SYSPSMT---
SSBP4_HUMAN             SNA--PGTPRDDGE-----MAAAGTFLHFPFSE-----SYSPGMT---
SSBP4_MOUSE            SNA--PGTPRDDGE-----MAAAGTFLHFPFSE-----SYSPGMT---

```

```

SSBP4_RAT NNA--PGTPRDDGE-----MAAAGTFLHFPFSE-----SYSPGMT---
SSBP3b_ZEBRAFISH SNP--PGTPRDE-D-----V--GGSYLHSFQNE-----NQYSPSMT---
SSBP3a_ZEBRAFISH SNP--PGTPRDDAE-----L--SGSFLHSFQNE-----NYSPTMT---
SSBP3_HUMAN SNP--PGTPRDDGE-----L--GGNFLHSFQND-----NYSPSMT---
SSBP3_MOUSE SNP--PGTPRDDGE-----L--GGNFLHSFQND-----NYSPSMT---
SSBP3_RAT SNP--PGTPRDDGE-----L--GGNFLHSFQND-----NYSPSMT---
Zgc:110158_ZEBRAFISH NNP--PGTPRDDGE-----M--GGNFLNPFQSE-----SYSPNMT---
SSBP4_ZEBRAFISH NNP--PGTPRDDGE-----M--AGNFLNPFQSE-----SYSPNMT---

```

```

FLO8_BUDDING_YEAST -----STNENQNVHSQNLKFGNIGMVED---QGPDYDLNLLDTNENDFNFINWEG---
ADN2_FISSION_YEAST SAPTESTTVATKSSDNQLLDVGNSTDIDAALLNDFDFDKFLKDTSTGDD---LWFGLFNL
Y53F4B.5_WORM -----
SAM-10_WORM -----GEISKIREGLLDG--FCA-----
SSDP_DROSOPHILA -----AAILKIKESMHEE--AKRFEKDTDHPD---YFMP-----
Si:ch211-130m23.3_ZEBRAFISH -----MSV-----
SSBP2_ZEBRAFISH -----MSV-----
SSBP42_RAT -----MSV-----
SSBP2_HUMAN -----MSV-----
SSBP2_MOUSE -----MSV-----
SSBP4_HUMAN -----MSV-----
SSBP4_MOUSE -----MSV-----
SSBP4_RAT -----MSV-----
SSBP3b_ZEBRAFISH -----MSV-----
SSBP3a_ZEBRAFISH -----MSV-----
SSBP3_HUMAN -----MSV-----
SSBP3_MOUSE -----MSV-----
SSBP3_RAT -----MSV-----
Zgc:110158_ZEBRAFISH -----MSV-----
SSBP4_ZEBRAFISH -----MSV-----

```

```

FLO8_BUDDING_YEAST -----
ADN2_FISSION_YEAST PDNEDSTAA
Y53F4B.5_WORM -----
SAM-10_WORM -----
SSDP_DROSOPHILA -----
Si:ch211-130m23.3_ZEBRAFISH -----
SSBP2_ZEBRAFISH -----
SSBP42_RAT -----
SSBP2_HUMAN -----
SSBP2_MOUSE -----
SSBP4_HUMAN -----
SSBP4_MOUSE -----
SSBP4_RAT -----
SSBP3b_ZEBRAFISH -----
SSBP3a_ZEBRAFISH -----
SSBP3_HUMAN -----
SSBP3_MOUSE -----
SSBP3_RAT -----
Zgc:110158_ZEBRAFISH -----
SSBP4_ZEBRAFISH -----

```

Curriculum Vitae

Dorota Michalski

M.Sc. Candidate
 Department of Biology
 The University of Western Ontario

EDUCATION:

M.Sc. Candidate, Cell and Molecular Biology 2015-Present
 Department of Biology, The University of Western Ontario

B.Sc. (Honors Specialization) Genetics and Biochemistry 2010-2015
 Department of Biology, The University of Western Ontario

HONOURS AND AWARDS:

Western Graduate Research Scholarship (WGRS) 2015-2017

Western Travel Award 2017

RELATED WORK EXPERIENCE:

Graduate Teaching Assistant 2015-2017
 The University of Western Ontario

PUBLICATIONS:

Farzad A., **Michalski D.**, and Karagiannis J. (2016) A Genetic Screen for Fission Yeast Gene Deletion Mutants Exhibiting Hypersensitivity to Latrunculin A. *G3: Genes, Genome, Genetics*, 6(10): 3399-3408.

CONFERENCES/PRESENTATIONS

Farzad A., **Michalski D.**, and Karagiannis J. A Genetic Screen for Fission Yeast Gene Deletion Mutants Exhibiting Hypersensitivity to Latrunculin A. Platform presentation: 9th International Fission Yeast Meeting May 14-19, 2017; Banff, AB.

Farzad A., **Michalski D.**, and Karagiannis J. A Genetic Screen for Fission Yeast Gene Deletion Mutants Exhibiting Hypersensitivity to Latrunculin A. Poster presentation: North East Regional Yeast Meeting June 16-17, 2016; Buffalo, NY.